

Observation of radio signals from an electron beam using an ice target

K. Mase, D. Ikeda, A. Ishihara, H. Sagawa, T. Shibata, M. Fukushima, T. Yamamoto, S. Yoshida, R. Gaior, K. Hanson, J. N. Matthews, T. Meures, B. K. Shin and G. B. Thomson, K. De Vries



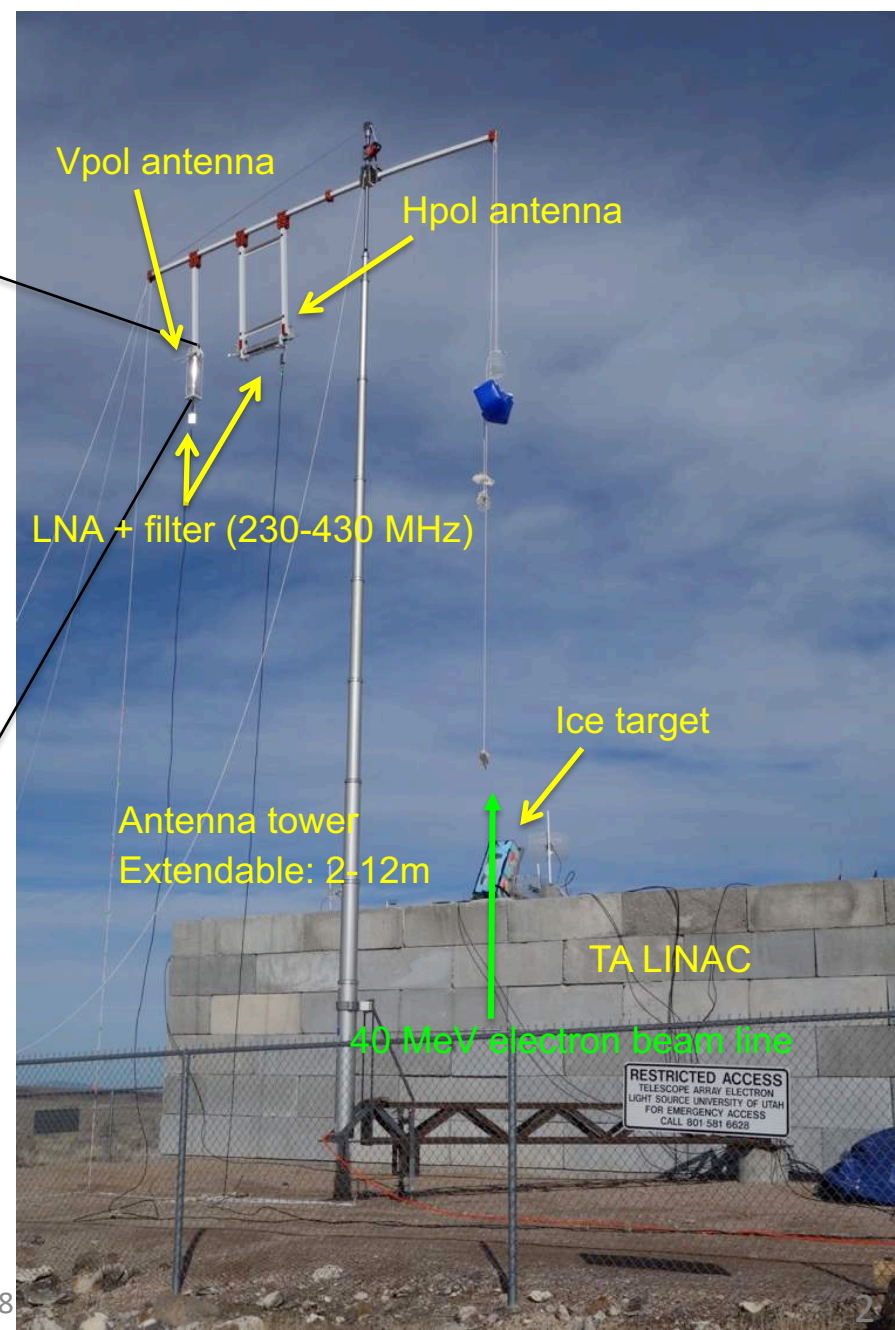
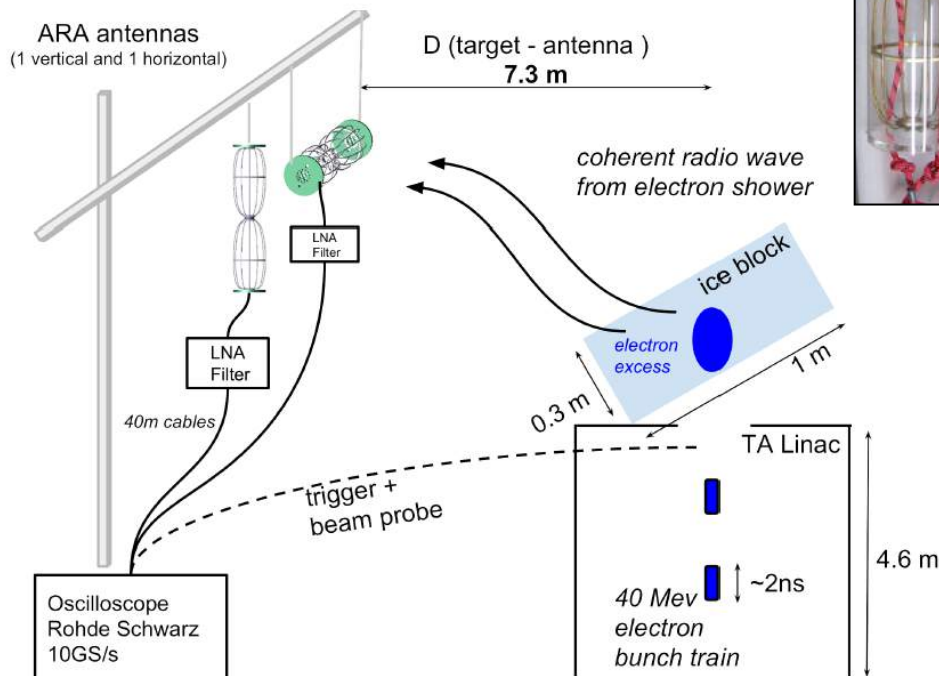
The ARA calibration with the TA-ELS (ARAcalTA)

Performed in January, 2015 at TA site, Utah

Purpose: Better understanding of the radio emissions and our detector

We measured

- ❖ Polarization
- ❖ Angular distribution
- ❖ Coherence

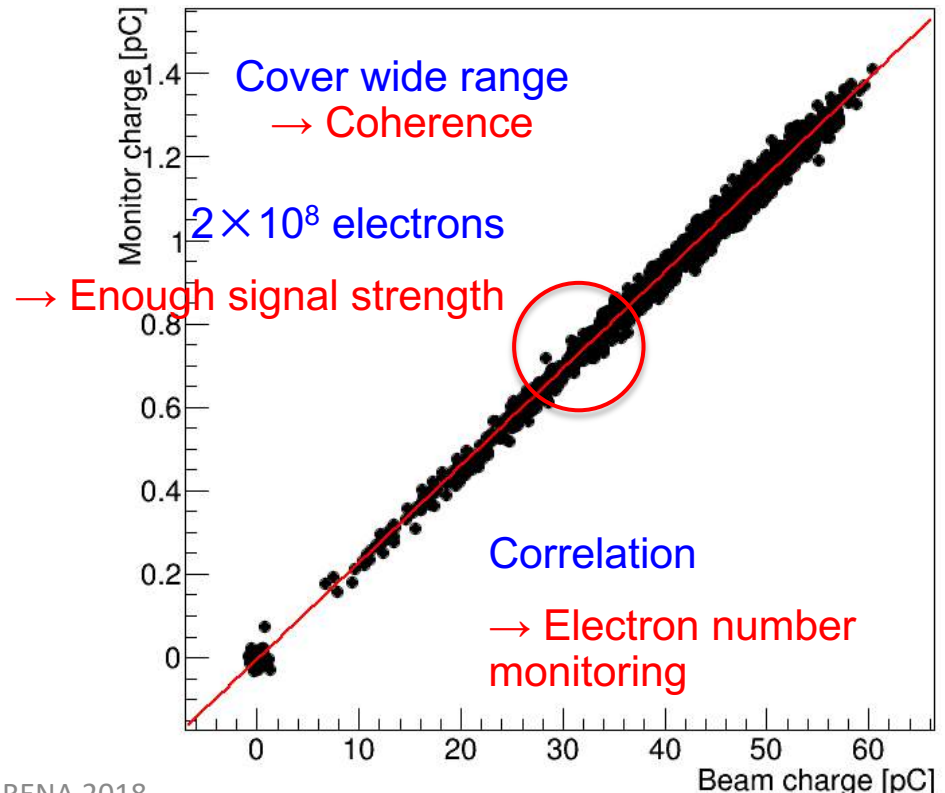
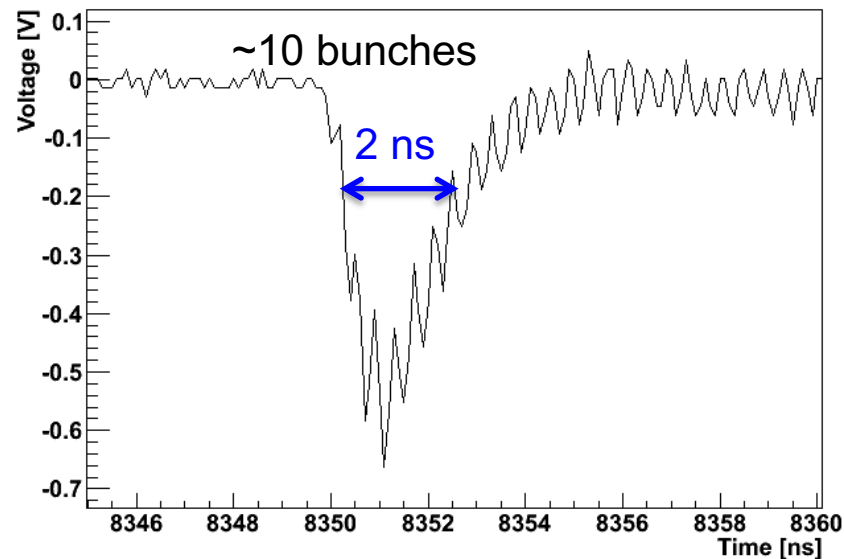


TA LINAC

- ✓ 40 MeV electron beam
- ✓ Typical electron number per bunch train:
 $2 \times 10^8 \rightarrow 30 \text{ PeV EM shower (shower length } \sim 20 \text{ cm)}$
- ✓ Pulse frequency: 2.86 GHz
→ pulse interval: 350 ps
- ✓ Bunch train width was optimized to ~ 2 ns
- ✓ Beam lateral spread: ~ 4.5 cm
- ✓ Trigger signal available
- ✓ Electron number can be monitored ($\sim 3\%$)

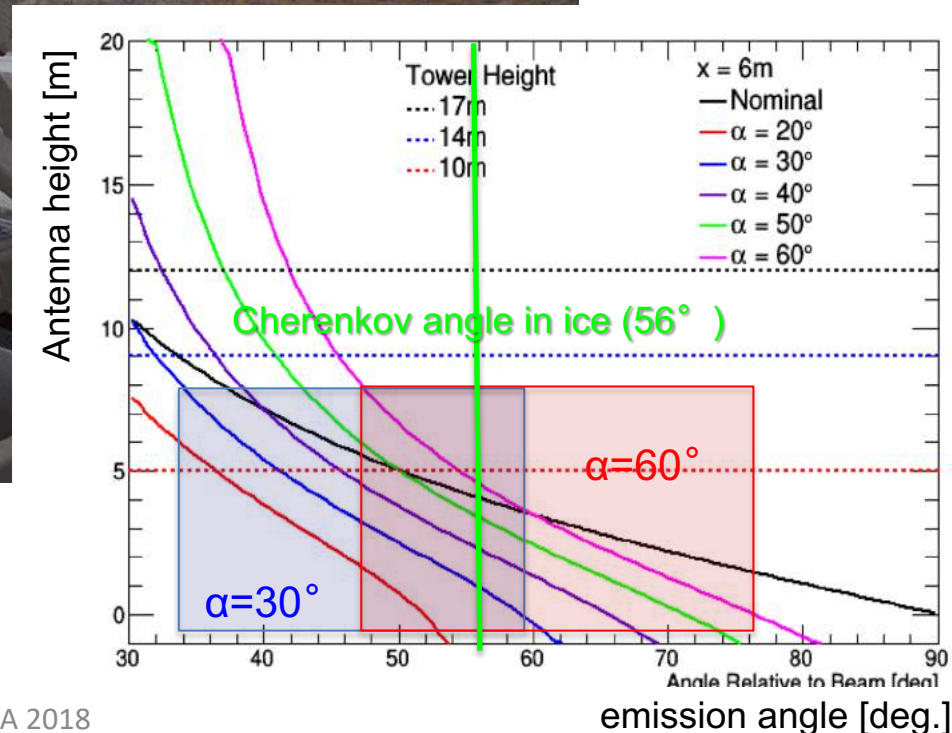
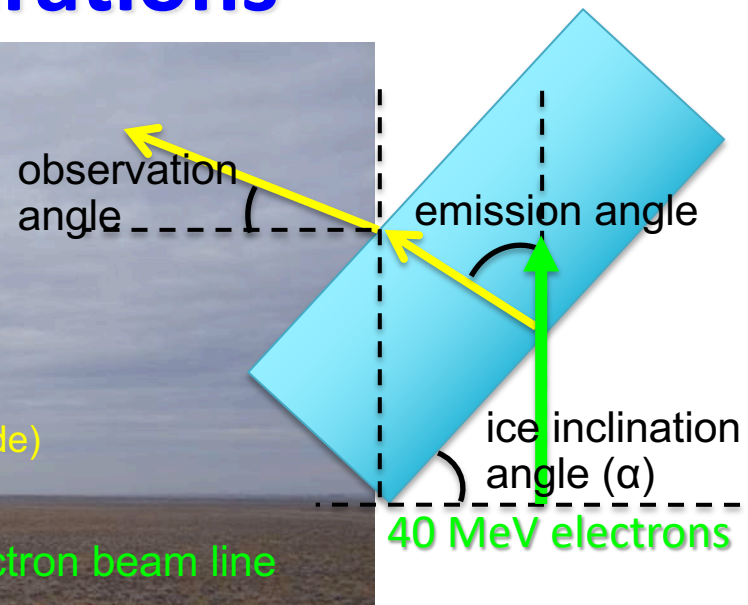
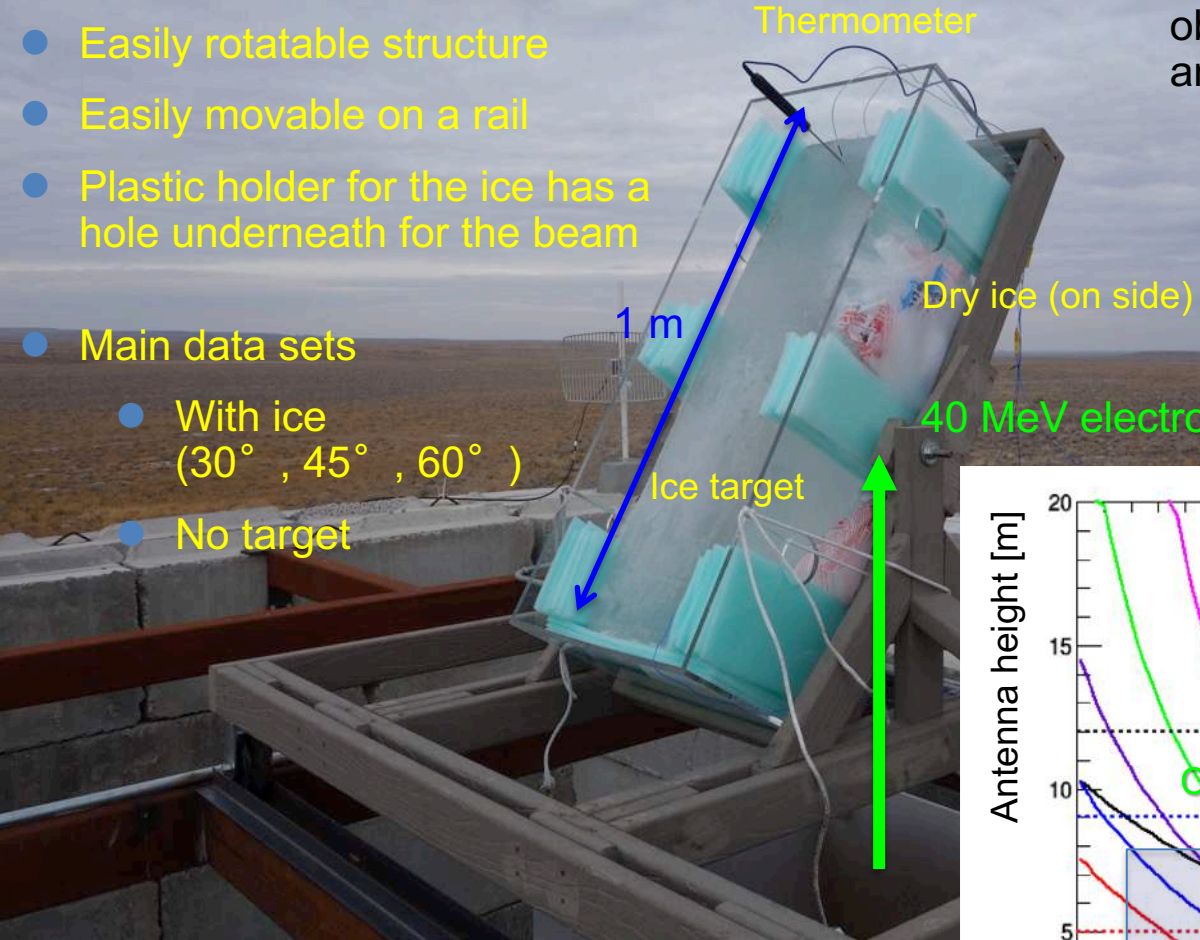


Measured bunch structure



Ice target and the configurations

- $100 \times 30 \times 30 \text{ cm}^3$
- Easily rotatable structure
- Easily movable on a rail
- Plastic holder for the ice has a hole underneath for the beam
- Main data sets
 - With ice (30° , 45° , 60°)
 - No target

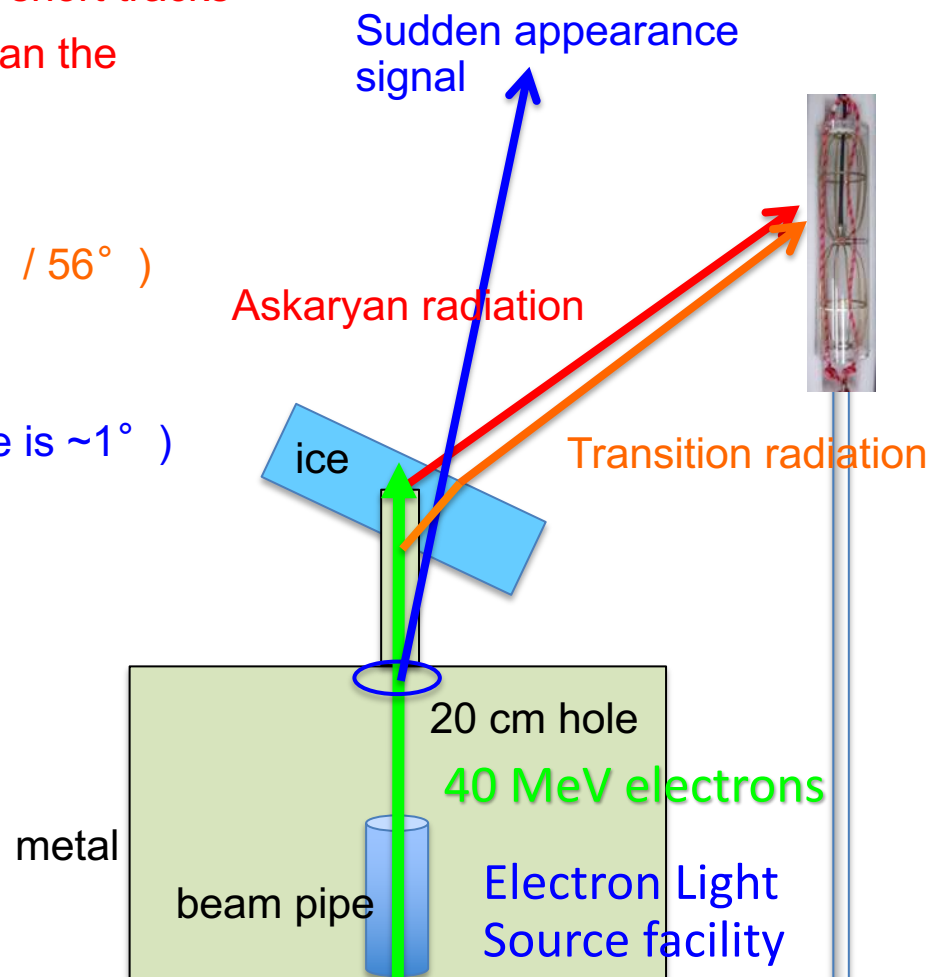


Expected radio emissions

- ✓ Several radio emissions are expected
 - ✓ Askaryan radiation
 - ✓ In ice
 - ✓ Wide angular distribution due to the short tracks
 - ✓ Peak at more horizontal direction than the Cherenkov angle (56°)
 - ✓ Transition radiation
 - ✓ At air/ice boundary
 - ✓ Peak at two Cherenkov angles ($\sim 1^\circ / 56^\circ$)
 - ✓ Sudden beam appearance radiation
 - ✓ When beam appears
 - ✓ Forward emission (Cherenkov angle is $\sim 1^\circ$)
- ✓ Originated from the same mechanism:
Lienard-Wiechert potential (for the moving particle)

$$\Phi(\vec{x}, t) = \left[\frac{e}{(1 - n\vec{\beta} \cdot \hat{r})R} \right]_{\text{ret}}, \quad \vec{A}(\vec{x}, t) = \left[\frac{e\vec{\beta}}{(1 - n\vec{\beta} \cdot \hat{r})} \right]_{\text{ret}},$$

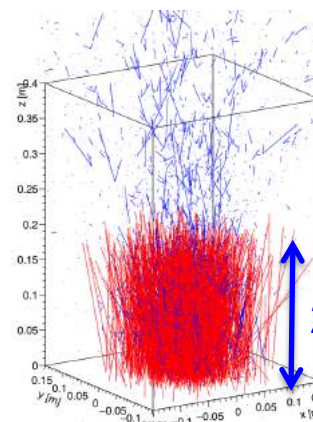
$$\mathbf{E} = -\nabla\phi - \frac{\partial \mathbf{A}}{\partial t}$$



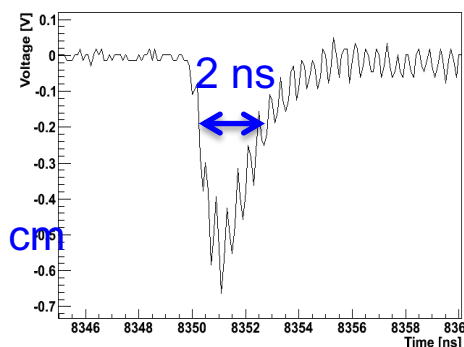
Simulation

Electron beam (Geant4)

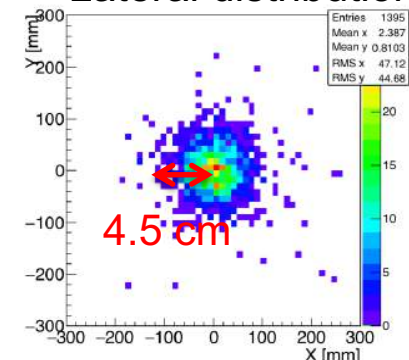
Including accelerator configurations



Bunch structure



Lateral distribution



E-field calculation

Based on the classical EM theory (Lienard-Wiechert potentials)

Middle point method (PRD 81, 123009 (2010))

Thanks to Anne Zilles for sharing her code for the implementation

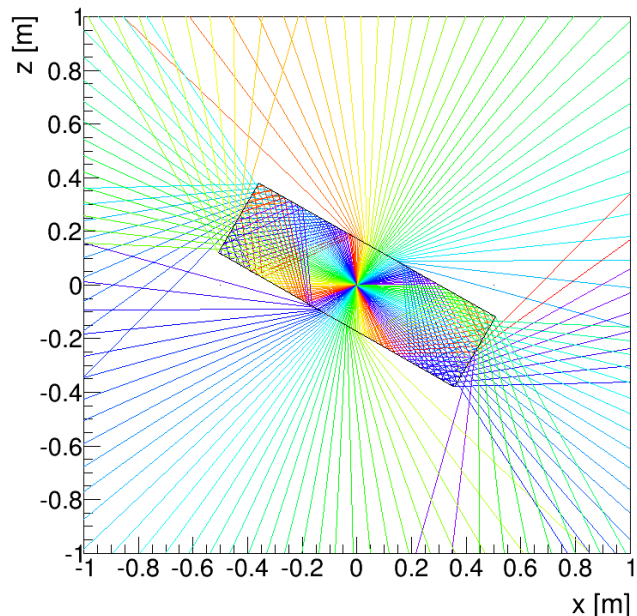
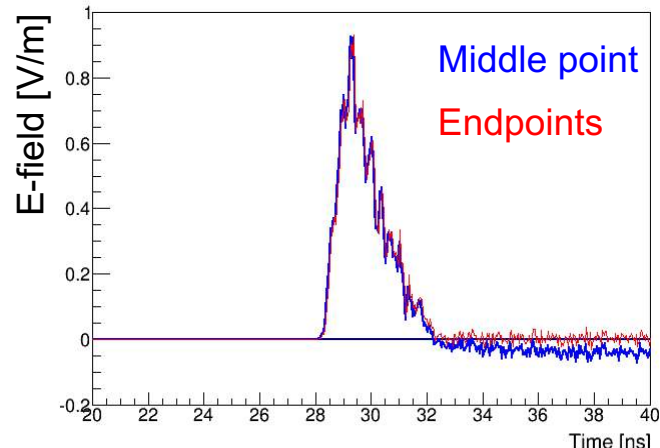
Endpoints method (PRE84, 056602 (2011))

tables made

E-field

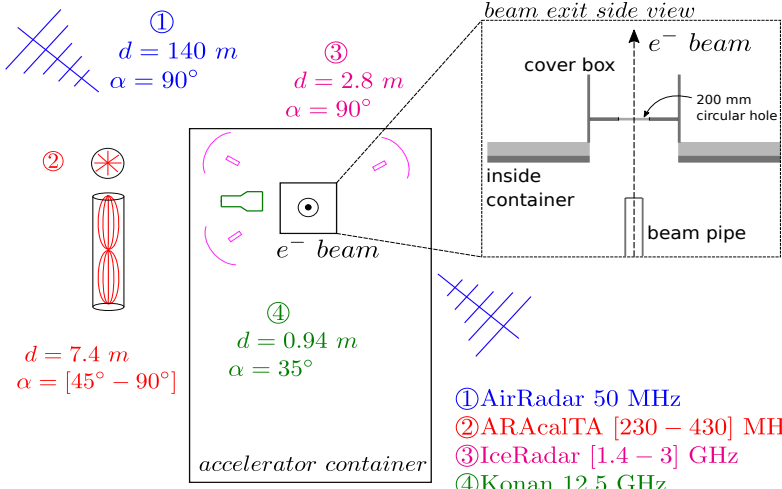
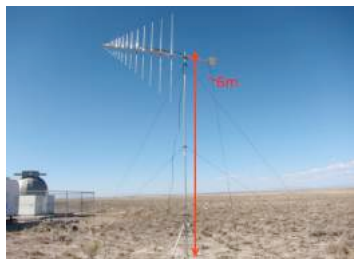
Detector response

Obs. angle 0° (no target) at 1 m



Sudden beam appearance signal

1. AirRadar



3. IceRadar

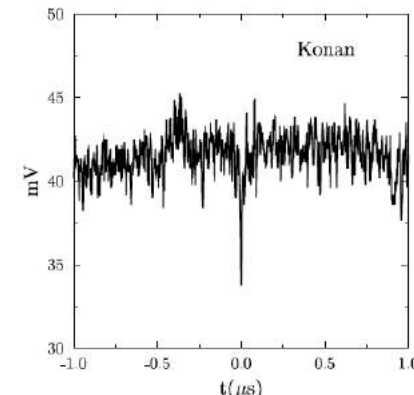
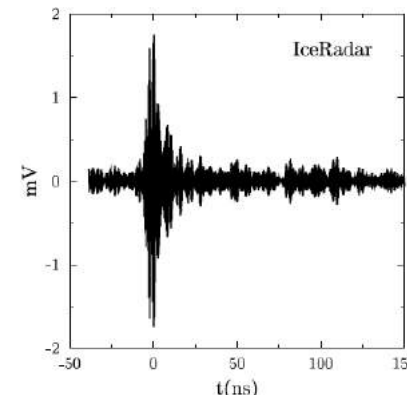
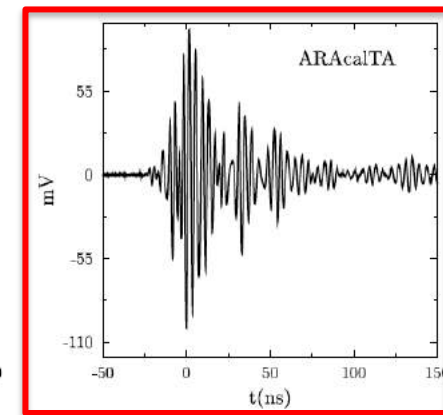
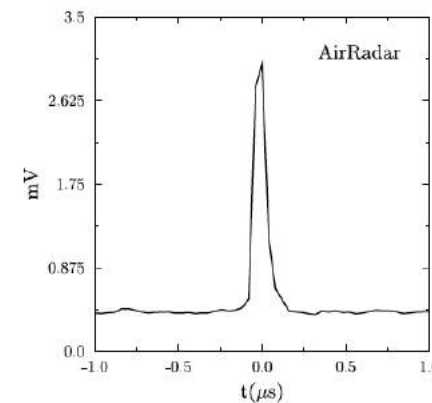


2. ARACalTA

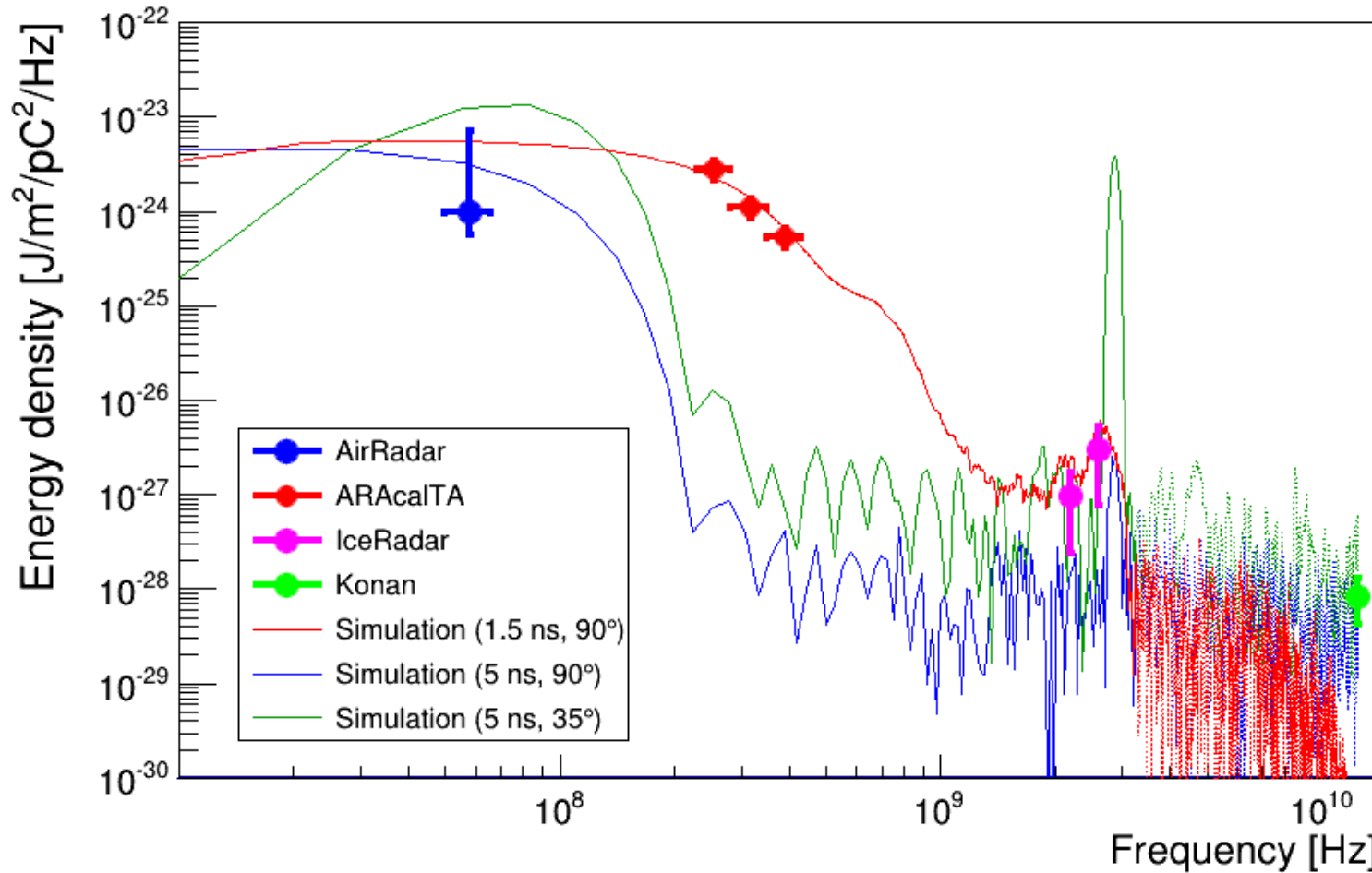


4. Konan

- ✓ Four independent experiments performed at the TA site
- ✓ All experiments clearly observed strong signals when beams appear

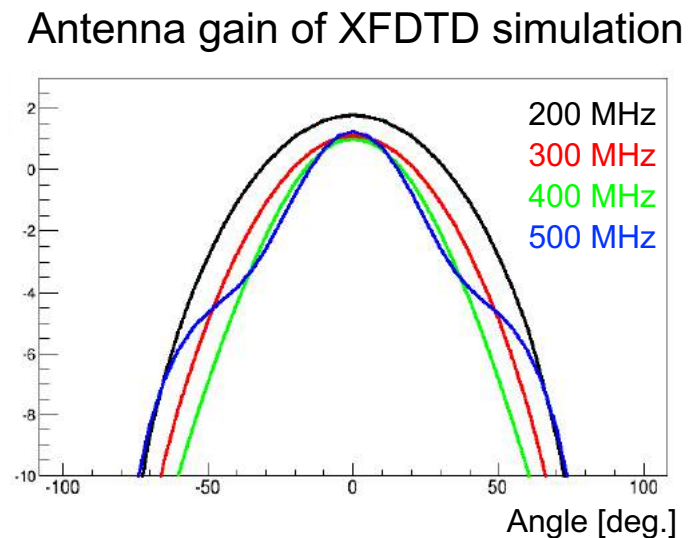
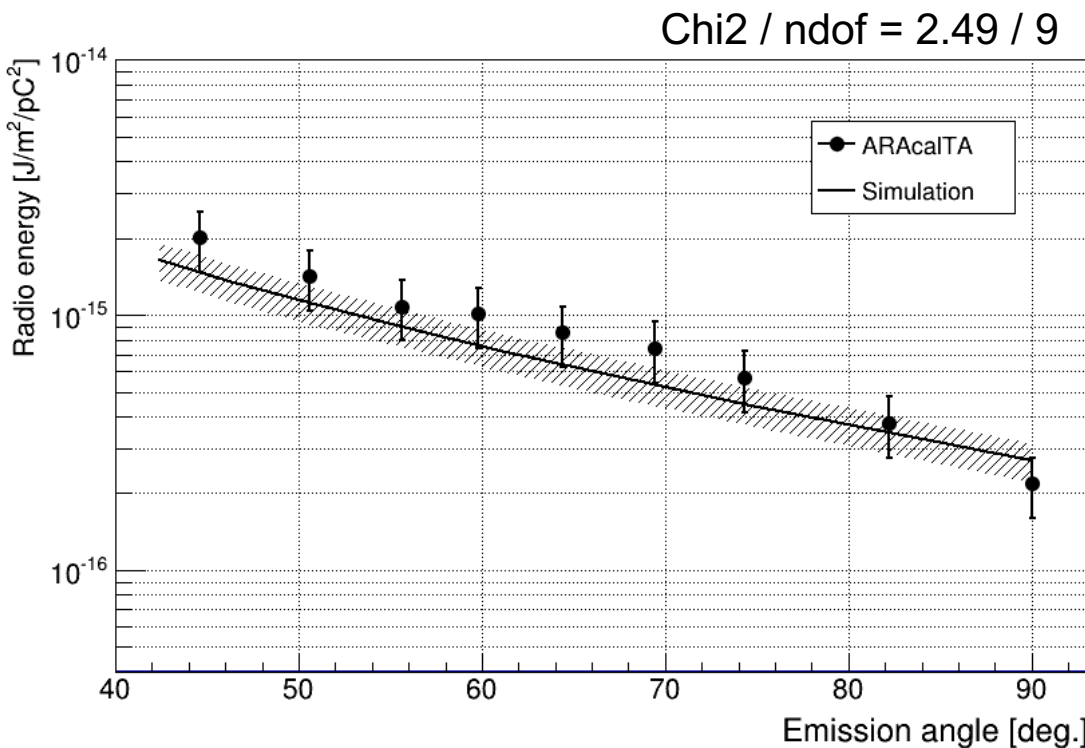


Frequency spectrum of the sudden beam appearance signals



- ✓ First result to show the consistency with the expectation for the wide frequency range
- ✓ Radiation well understood
- ✓ Applicable for the UHECR detection

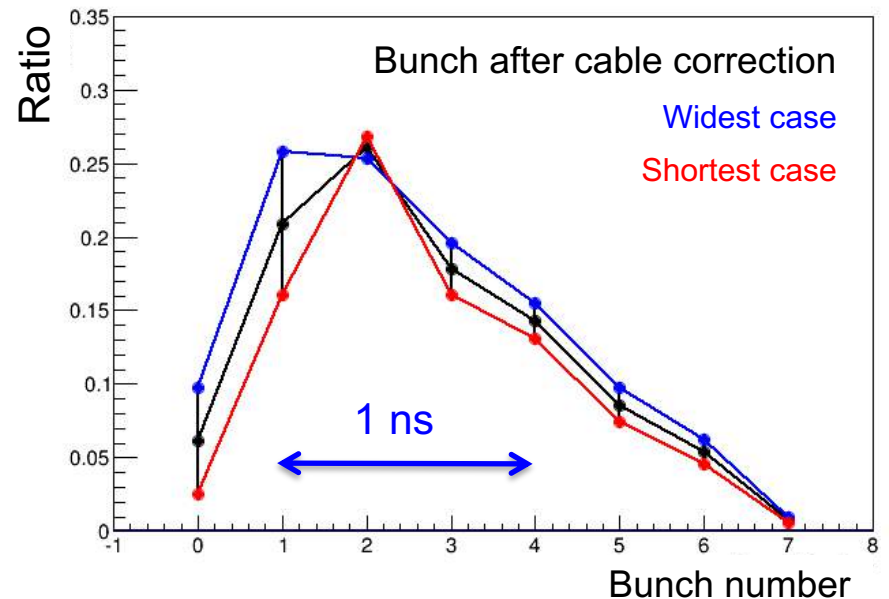
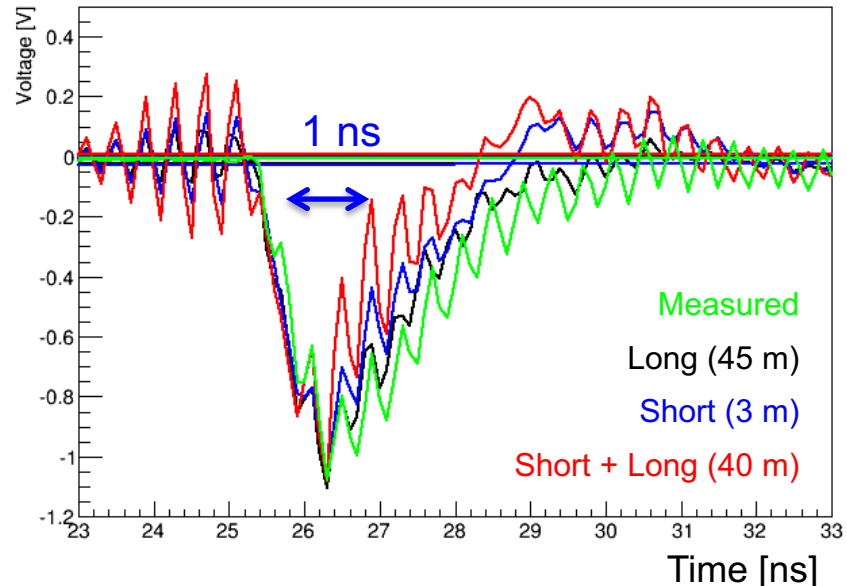
Angular distribution of the sudden beam appearance signals



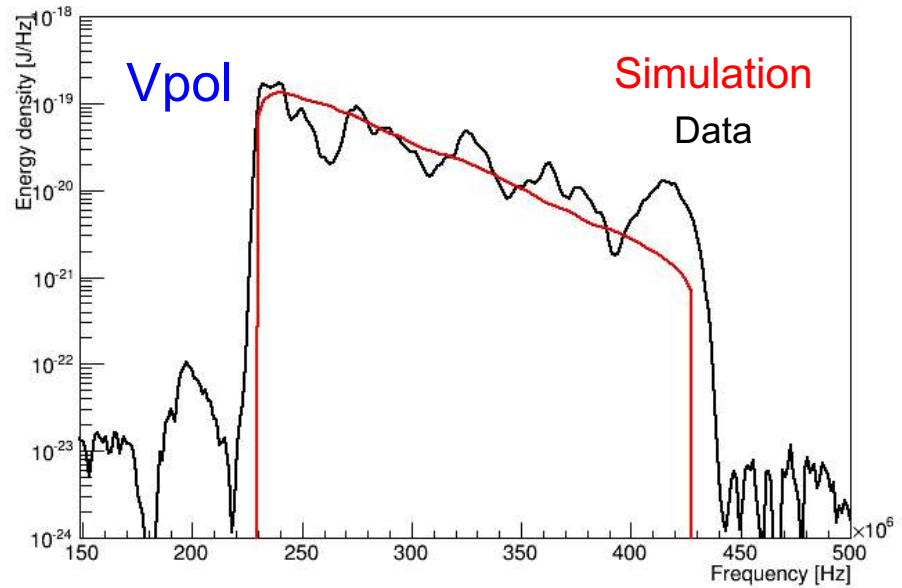
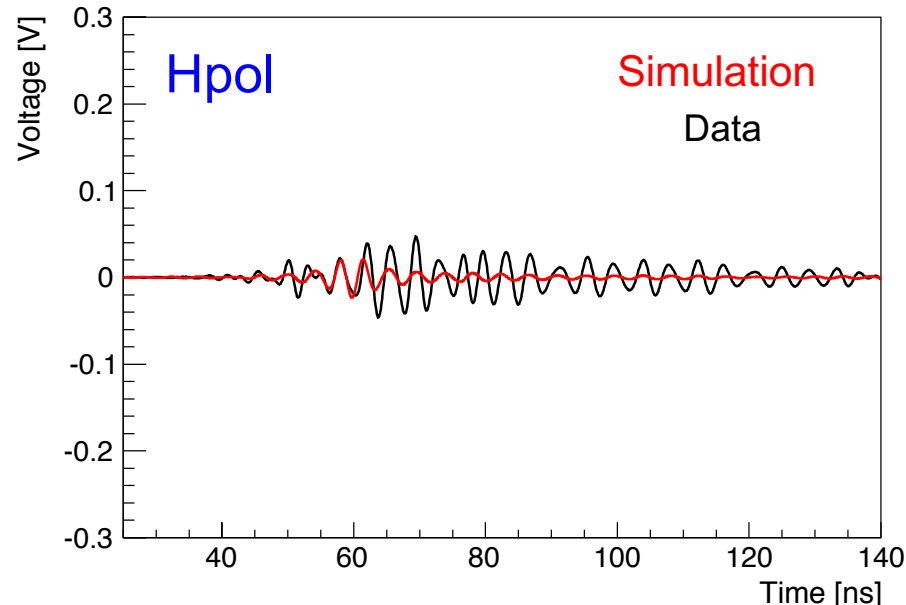
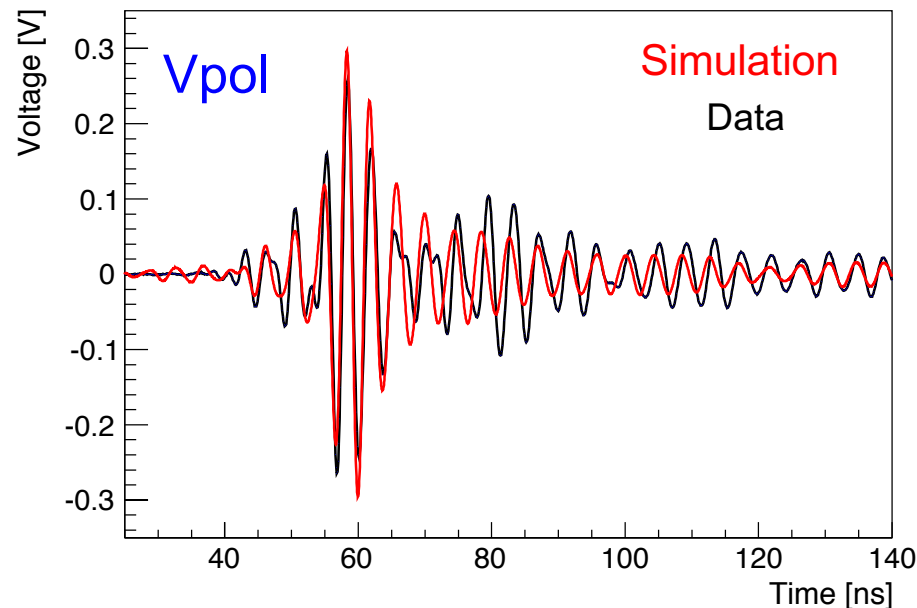
- ✓ Reasonable agreement between data and simulation (XFDTD)
- ✓ Radiation and our detector are well understood (level of 30%)

Systematic uncertainties

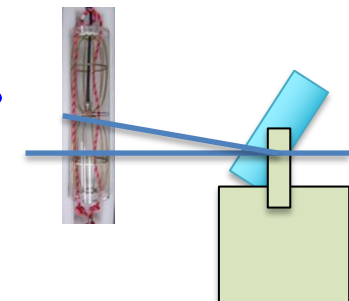
Item	Data	Simulation
Statistical error	$\pm 8\%$	$\pm 10\%$
Stability	$\pm 19\%$	-
Bunch width	-	-14% +17%
Sum	$\pm 21\%$	-17% + 20%



Signals with an ice target



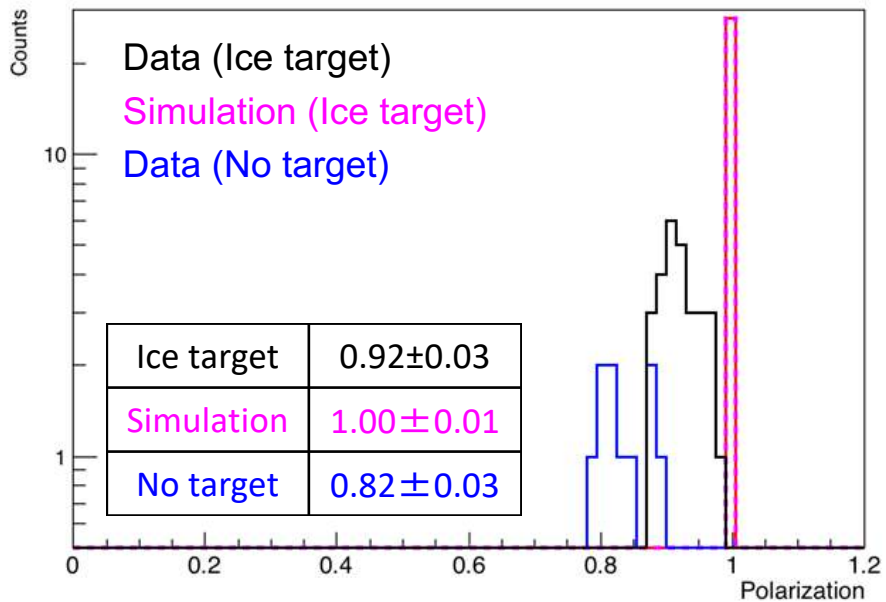
Configuration:
Ice 60° , obs. angle: 15°



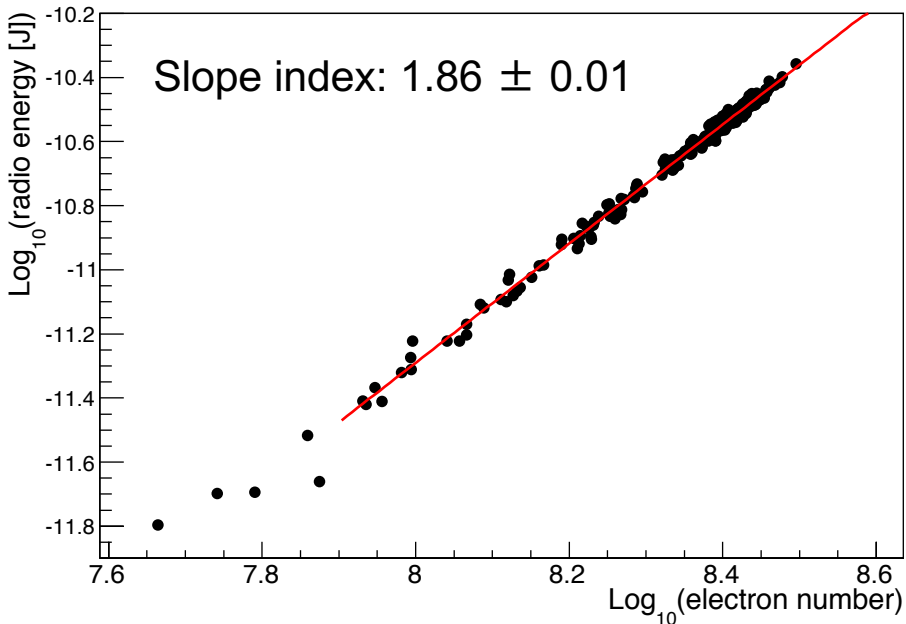
- ✓ Reasonable agreements between data and simulation
- ✓ Less Hpol signal → **high polarization**

Polarization and coherence

Polarization



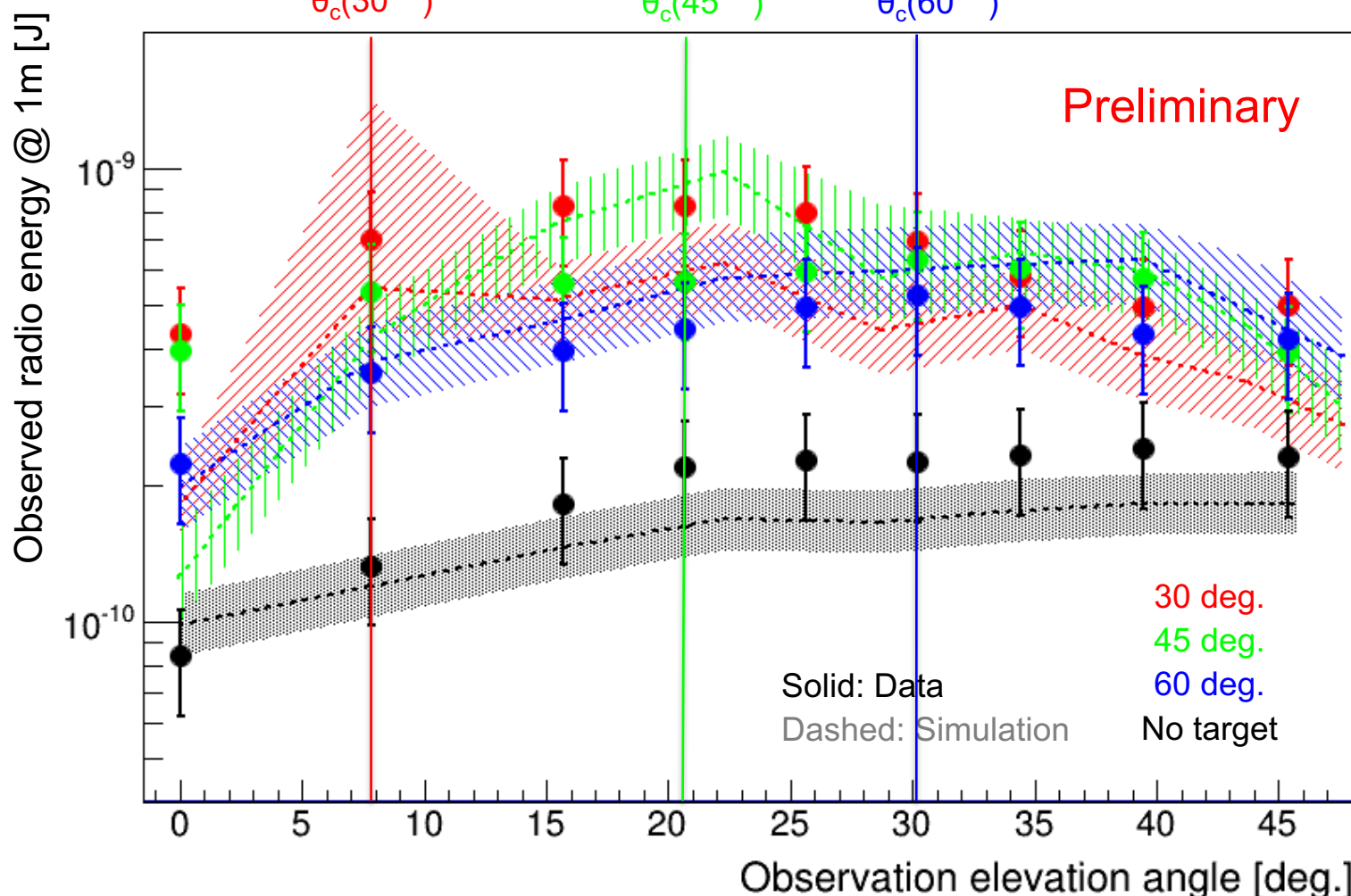
Configuration: Ice 30° , obs. angle 0° , Vpol



- ✓ All signals shows relatively high vertical polarization

- ✓ Reasonable coherence
- ✓ Similar values for all the configurations

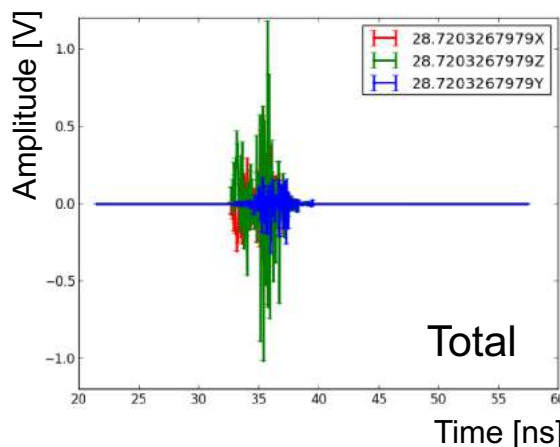
Angular distribution



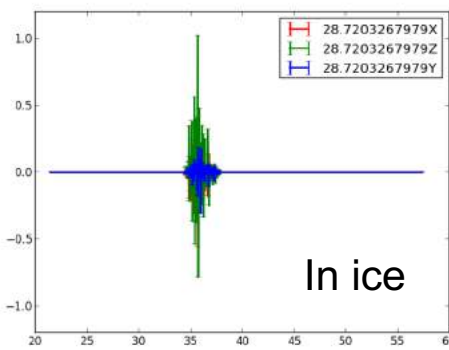
- ❖ Reasonable agreements
- ❖ Detector effects included in simulation
- ❖ Need to be changed to radio energy vs emission angle

Each component

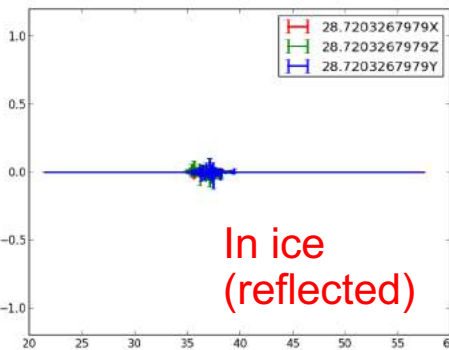
Preliminary



Total

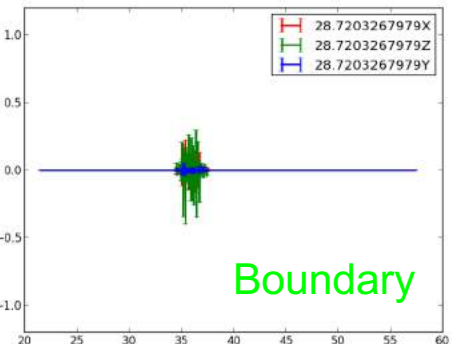
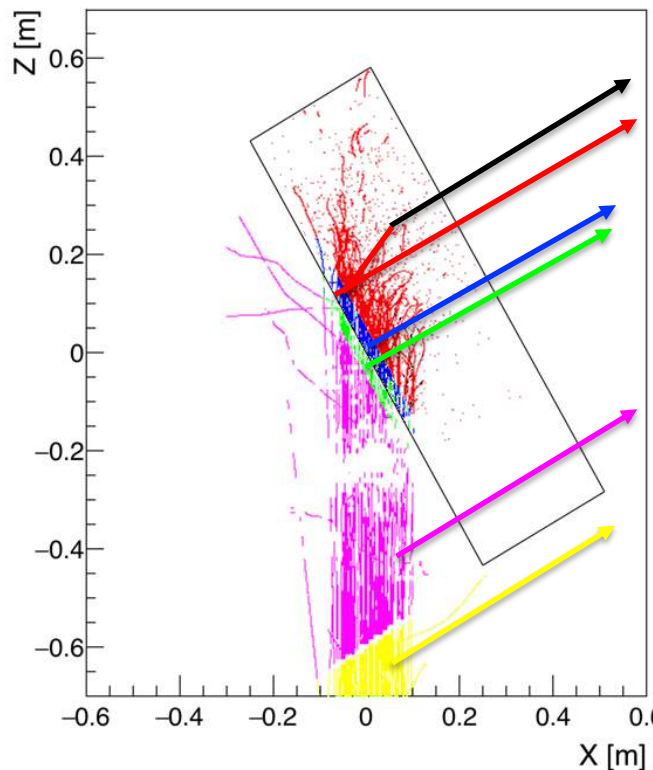


In ice

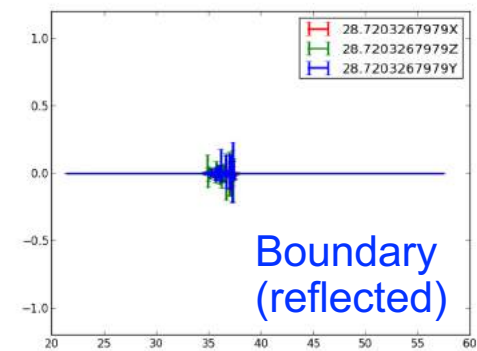


In ice
(reflected)

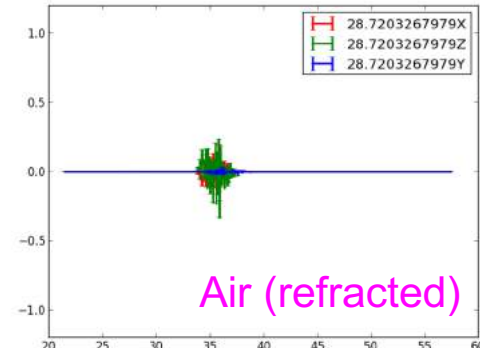
Configuration:
Ice 60° , obs. angle: 29°



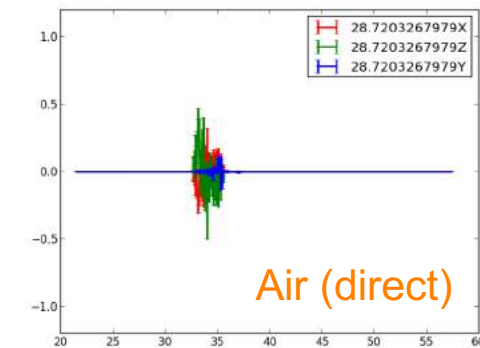
Boundary



Boundary
(reflected)



Air (refracted)



Air (direct)

■ Summary

- ✓ Performed experiments using an accelerator to verify the understanding of the radio signals as well as our detectors
- ✓ Clearly polarized and coherent signals observed
- ✓ Observed signals are consistent with the expectation within the uncertainty level of 30%
- ✓ Understanding the emission further by checking each component
- ✓ Would be important for sudden deaths of air showers

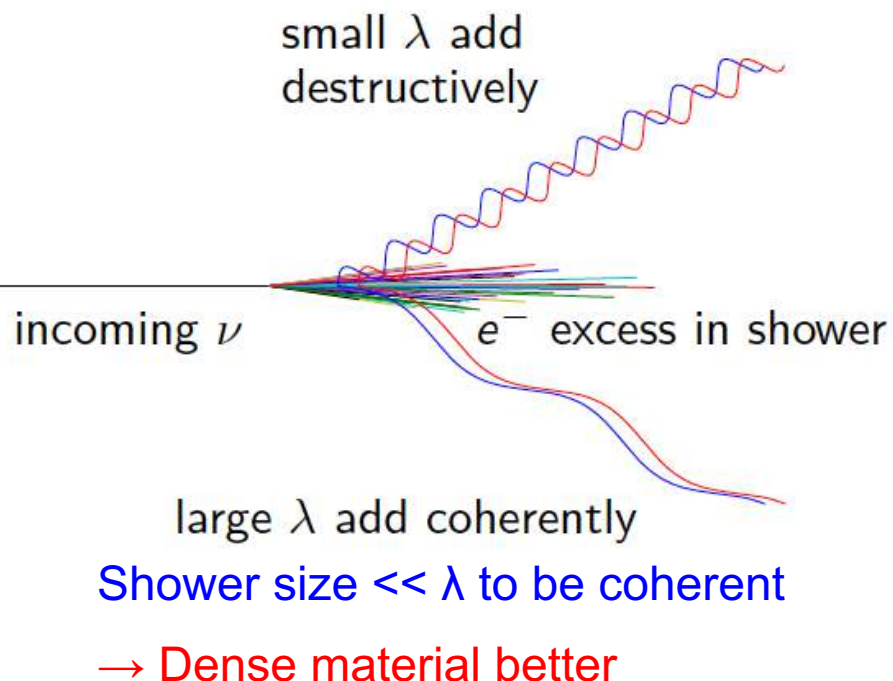
Backups

Askaryan effect

- 1962: Askaryan predicted coherent radio emission from excess negative charge in an EM shower
→ Askaryan effect



G. Askaryan



Cherenkov emission (Frank-Tumm result)

$$\frac{d^2W}{d\nu dl} = \frac{4\pi^2\hbar}{c} \alpha z^2 \nu \left(1 - \frac{1}{\beta^2 n^2}\right)$$

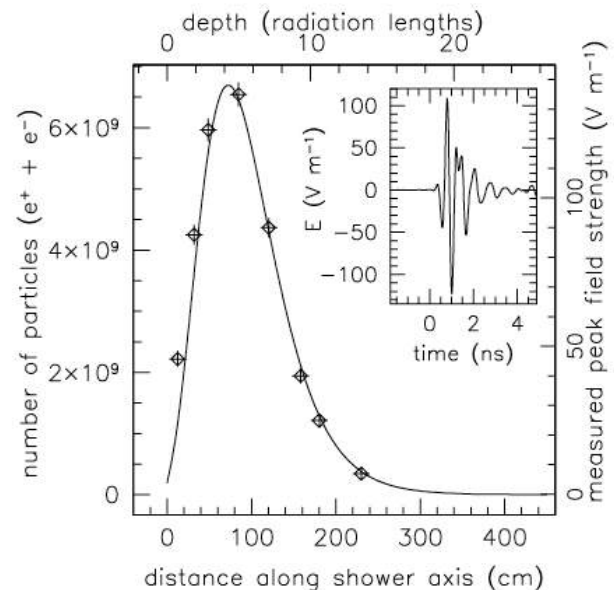
in case N electrons,
 $z=1$ (not coherent) → $W \propto N$
 $z=N$ (coherent) → $W \propto N^2$

Power $\propto \Delta q^2 \propto E^2$, thus prominent at ultra-high energy ($>\sim 100$ PeV)

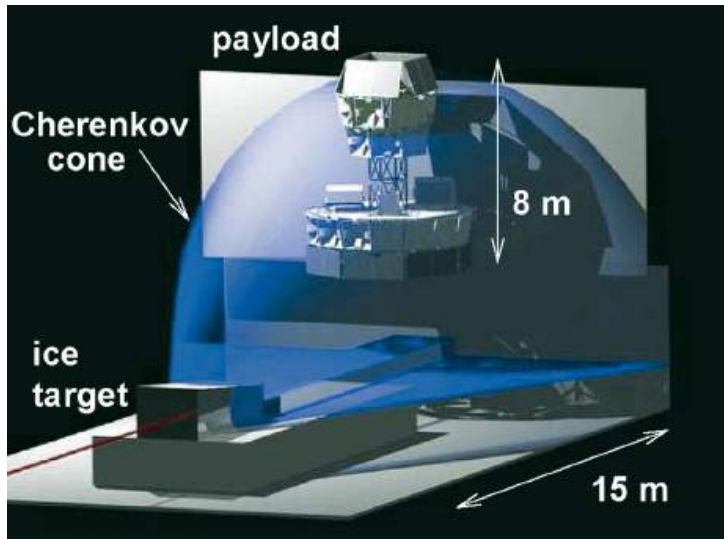
Verification of the Askaryan effect

- Askaryan effect has been verified using an accelerator
 - 2001: firstly confirmed at SLAC with Silica sand (D. Saltzberg et al.)
 - 2005: confirmed with salt (P. Gorham et al.)
 - 2007: confirmed with ice (P. Gorham et al.)

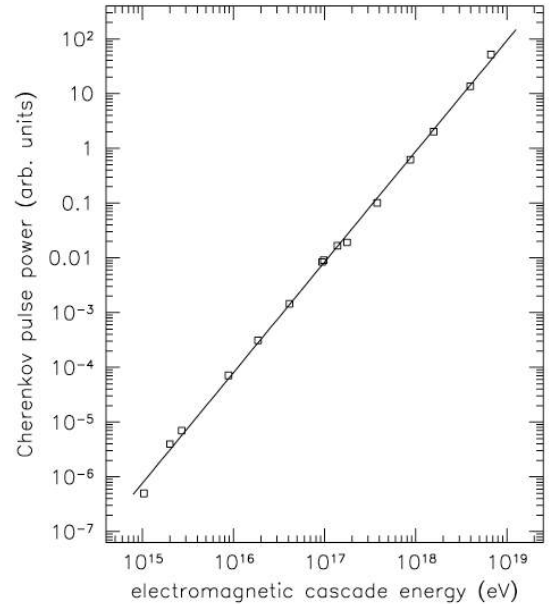
Saltzberg et al. PRL 2001



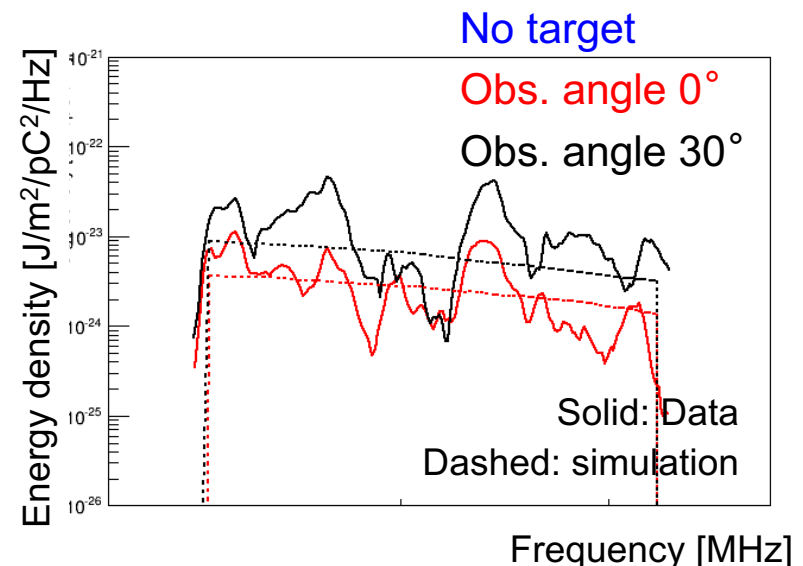
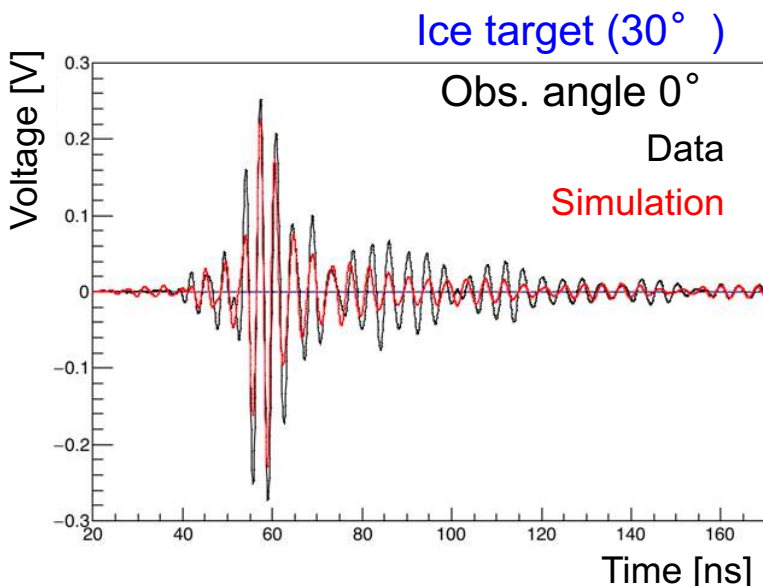
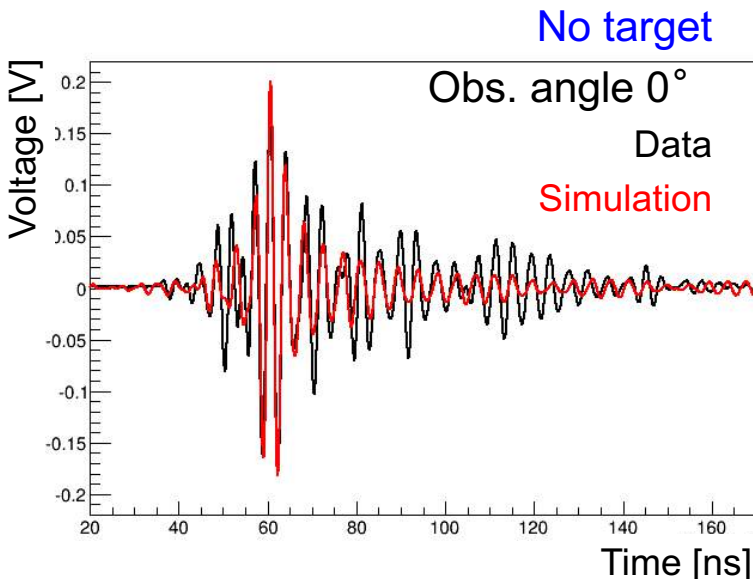
Gorham et al. PRL 2007



Gorham et al. PRD 2005

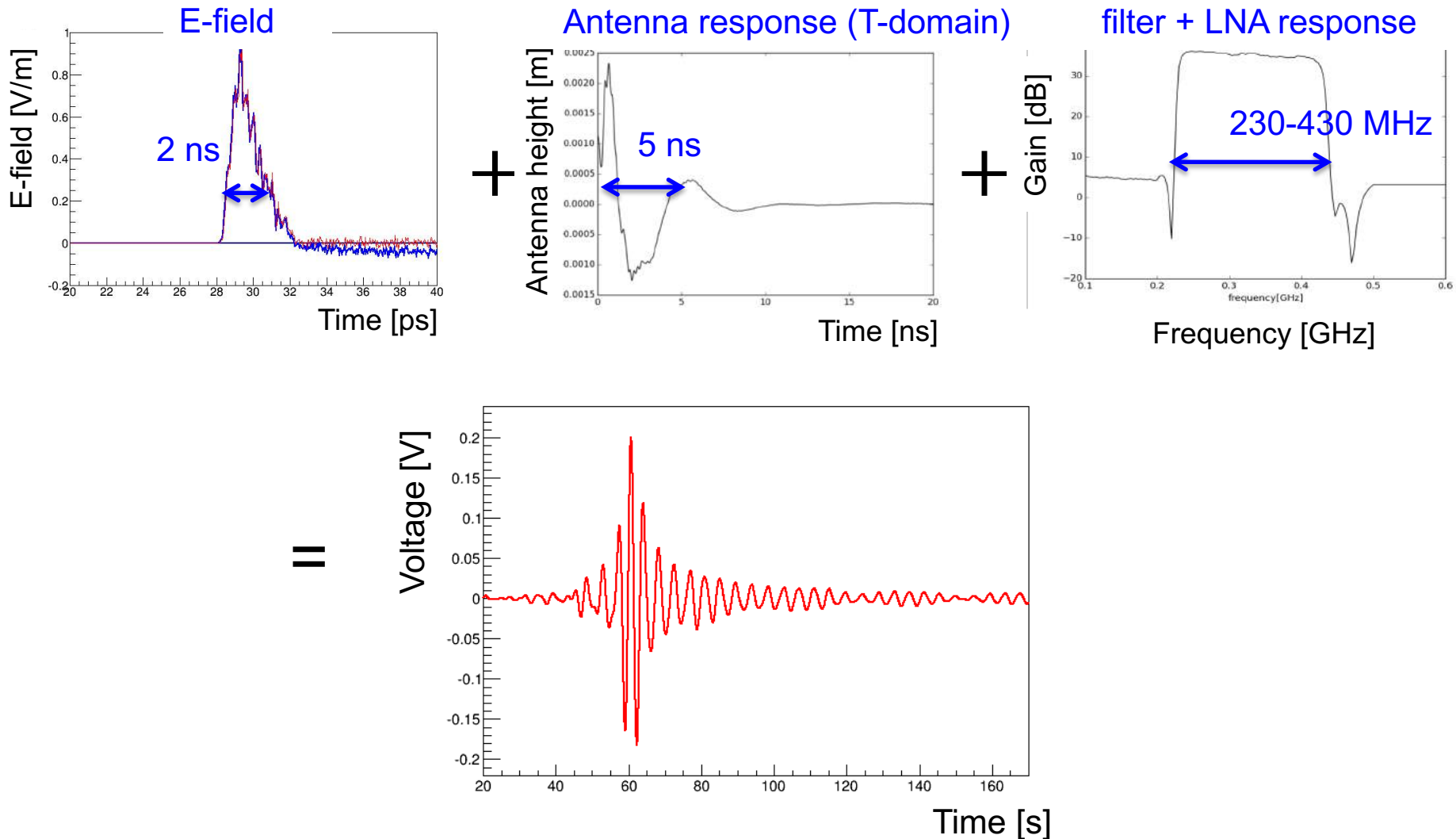


Comparison of waveforms and frequency spectrum



Reasonable agreements without scaling!

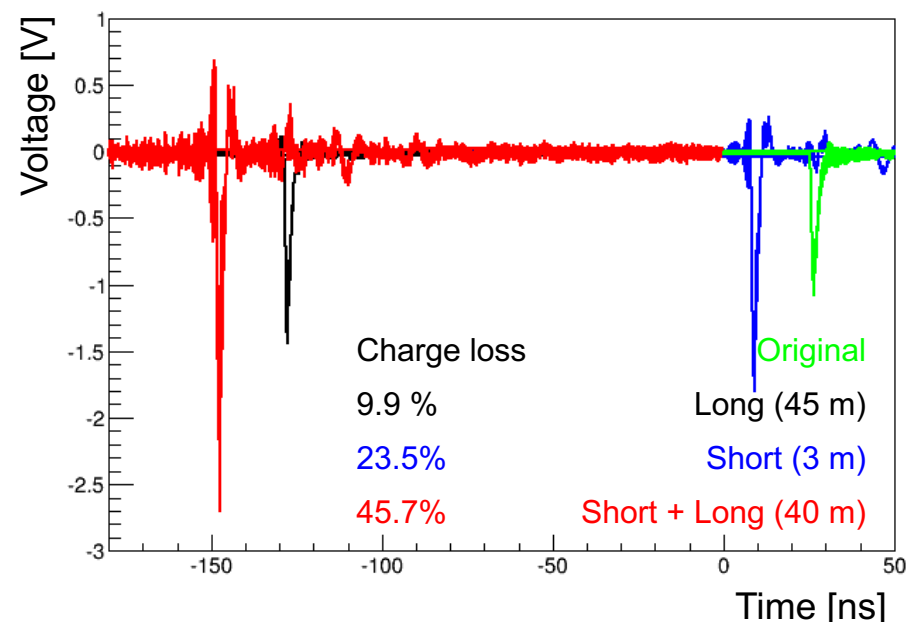
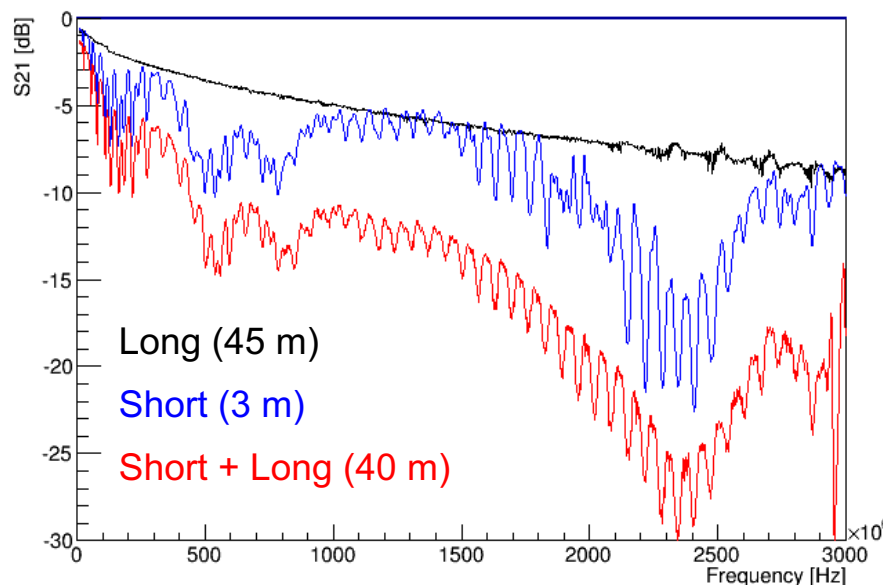
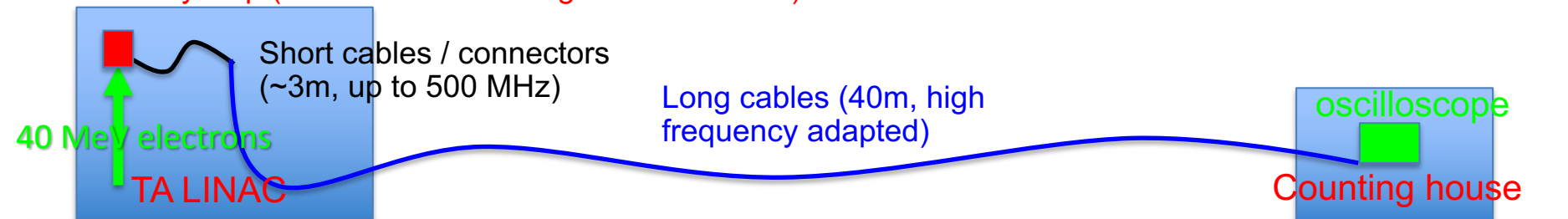
Detector simulation



Verify the understanding the emission mechanisms and detector responses, comparing with data

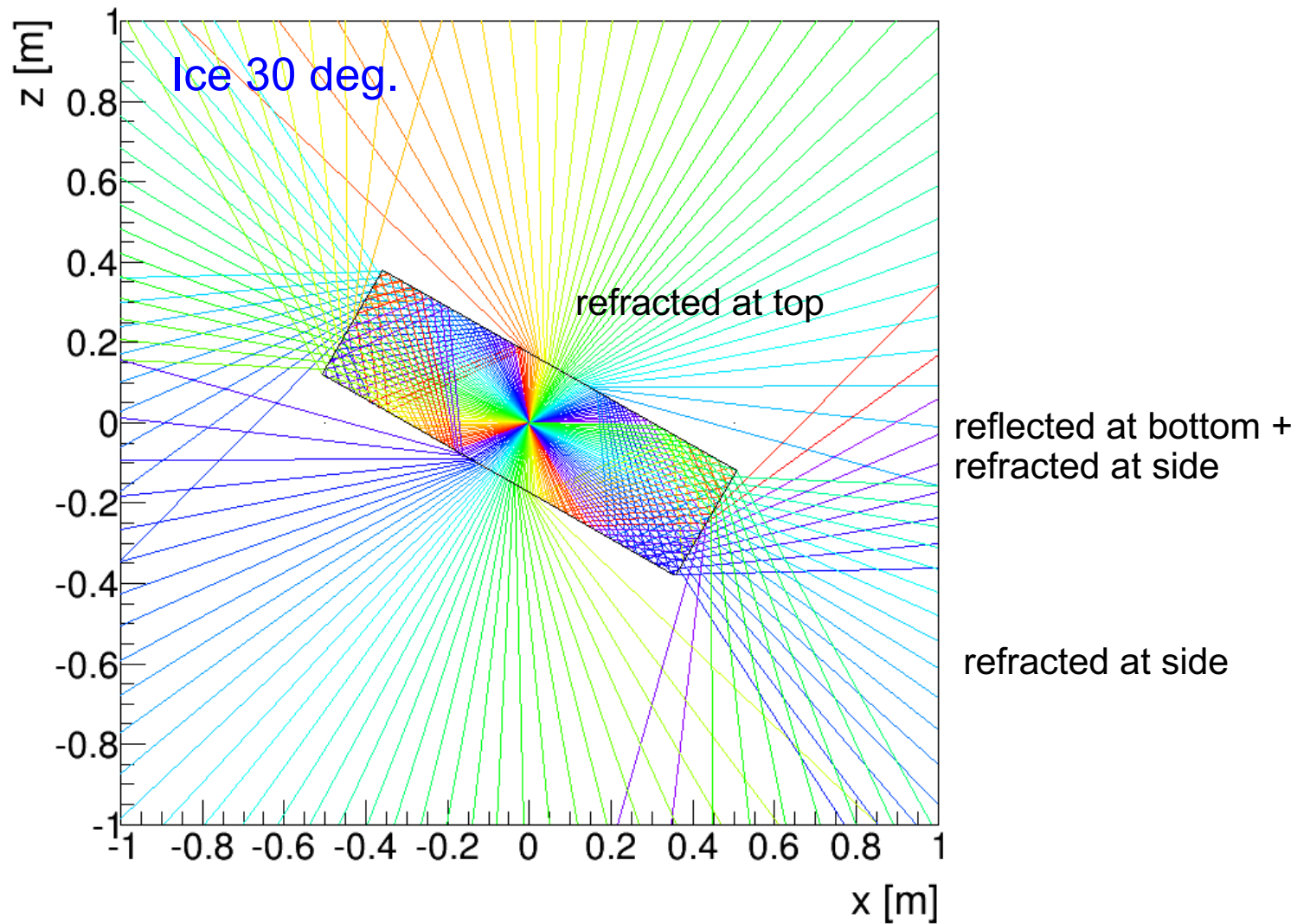
Cable / connector attenuation correction

Faraday Cup (for the electron charge measurement)



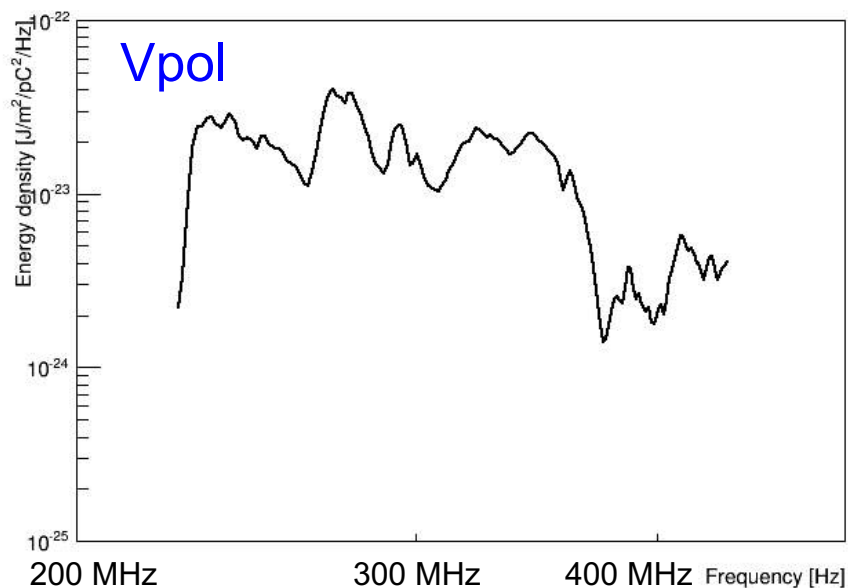
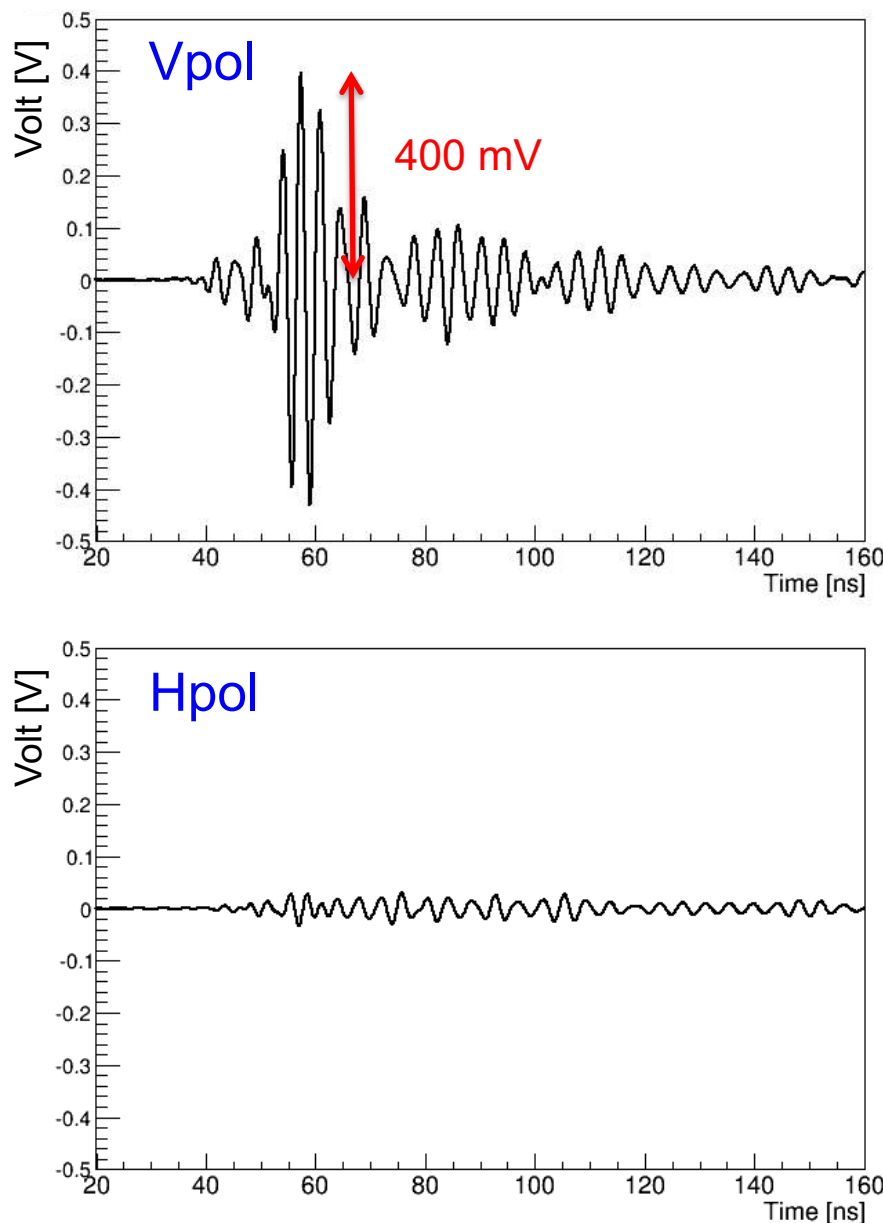
- ❖ Found out the TA short cable attenuate signal significantly
- ❖ The emission power is proportional to the charge square → correction of x2.1 (1.46^2)

■ Ray trace for emissions in ice

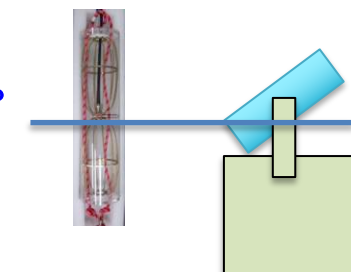


- ❖ Complicated...
- ❖ Need a full simulation (with lookup tables)

Measured waveform and the frequency spectrum



Configuration:
Ice 30° , obs. angle: 0°

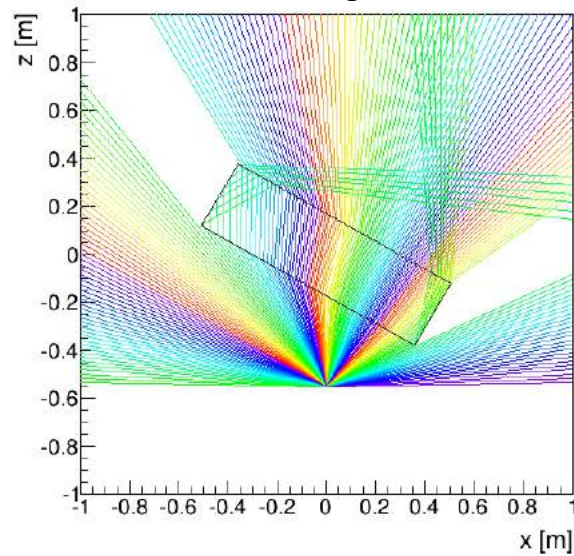


- ✓ Relatively large signal observed
- ✓ Less Hpol signal → high polarization
- ✓ Relatively flat frequency spectrum
→ Indicating something else from Askaryan radiation

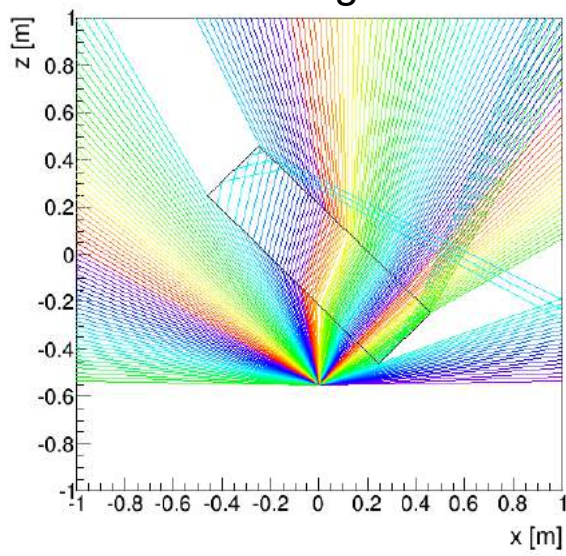
Ray traces

More shadowing effect for 30 deg. and 45 deg.
above observation angle of 30 deg.

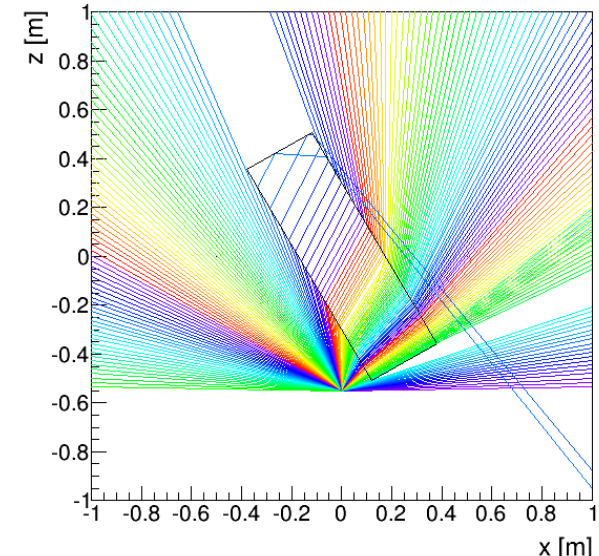
30 deg.



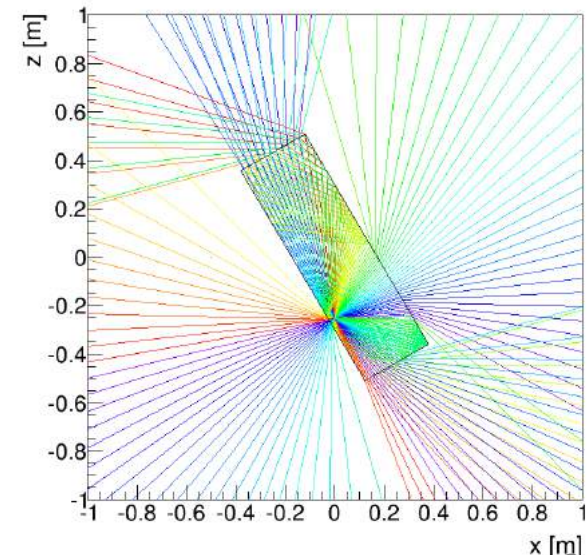
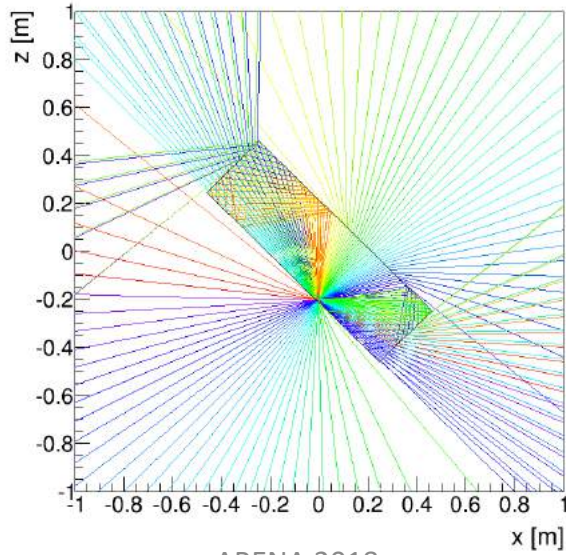
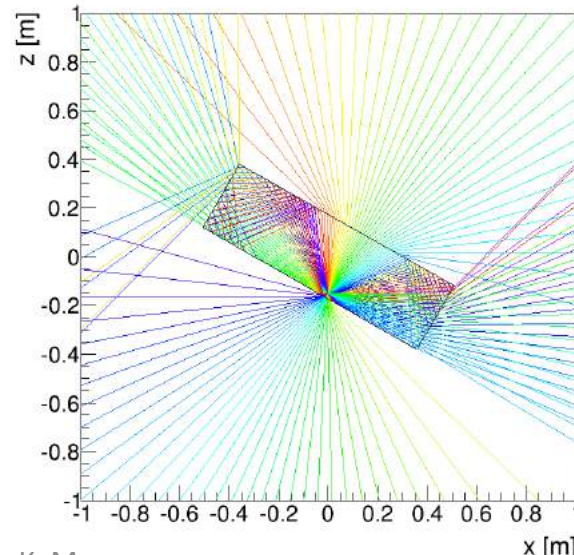
45 deg.



60 deg.



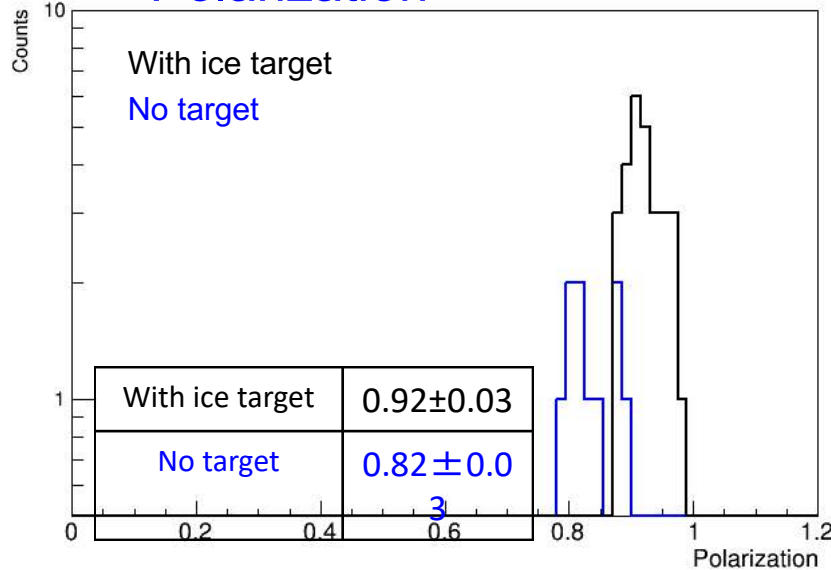
More signals for 30 deg. and 45 deg.



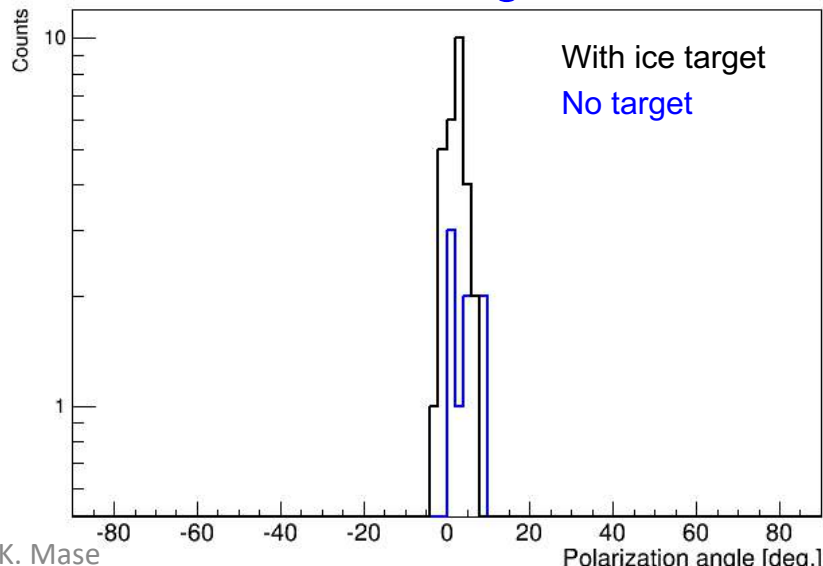
Properties of the signals

Configuration:
Ice angle 30° , obs. angle: 0°

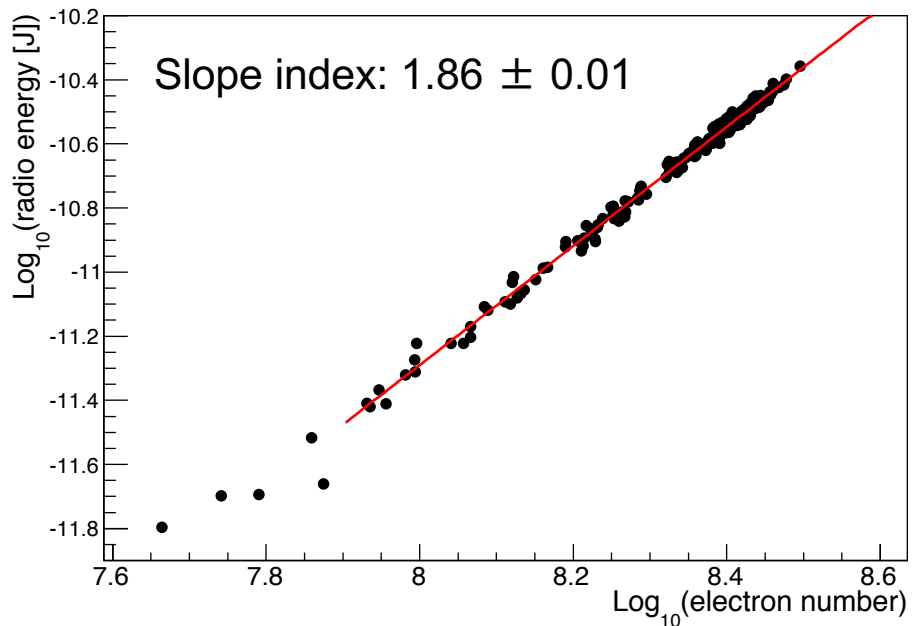
Polarization



Polarization angle



Coherence

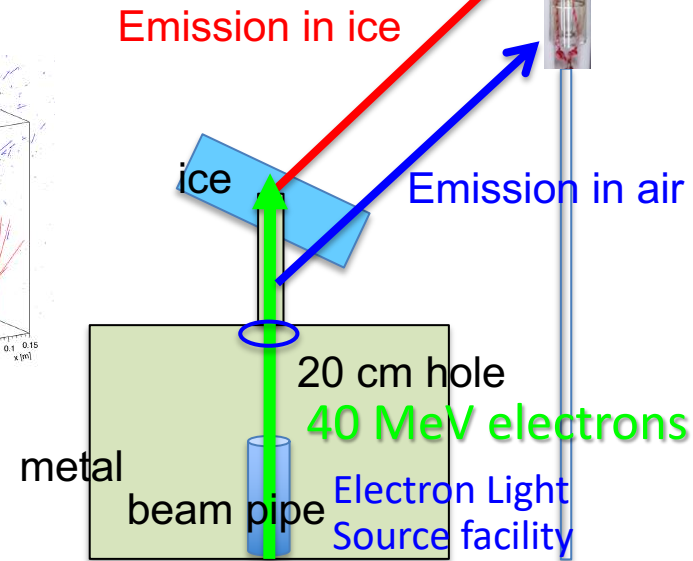
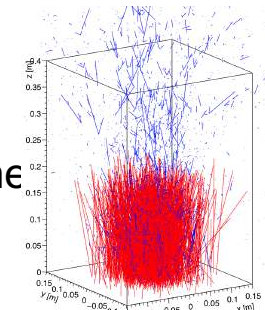


- ✓ All signals shows high vertical polarization
- ✓ No target data shows slightly less polarization
- ✓ High coherence, but not full

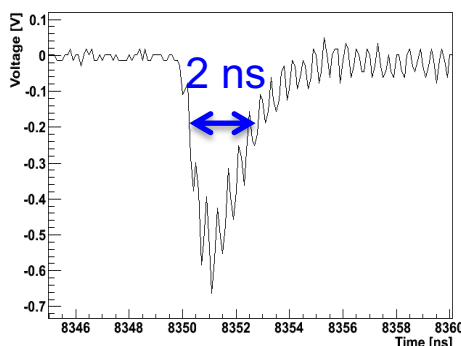
Simulation

- ✓ Electron beams simulated by Geant4
- ✓ Accelerator configurations included
- ✓ E-field calculated by the middle point method (ZHS method, PRD 81, 123009 (2010)) and the endpoints method (PRE84, 056602 (2011))

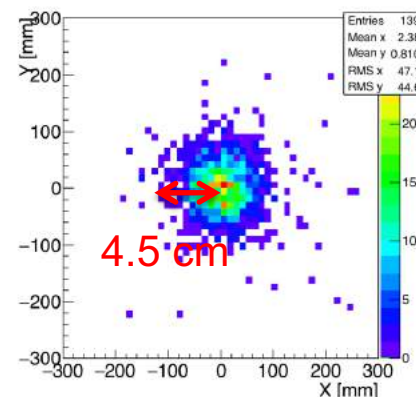
→ Both methods give the same results



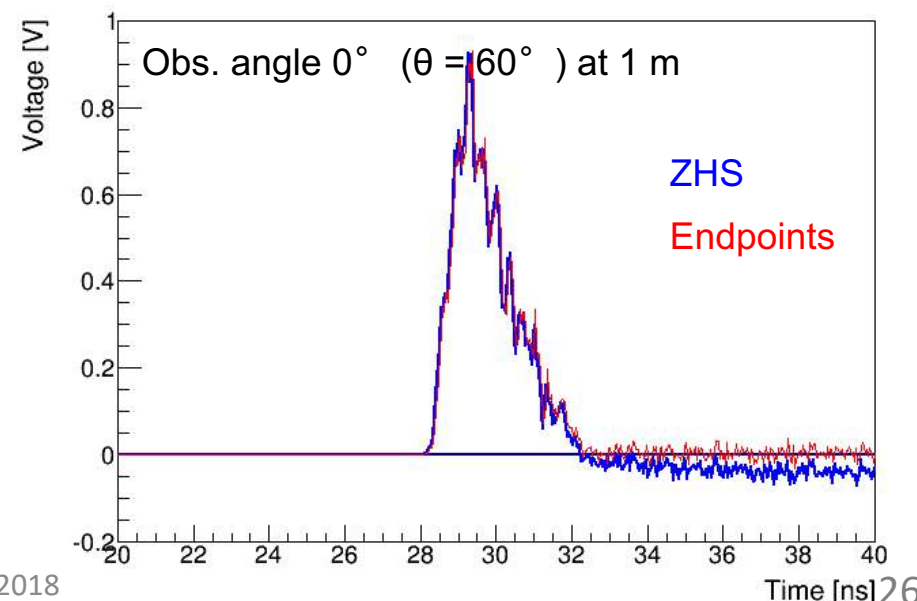
Bunch structure



Lateral distribution



ARENA 2018



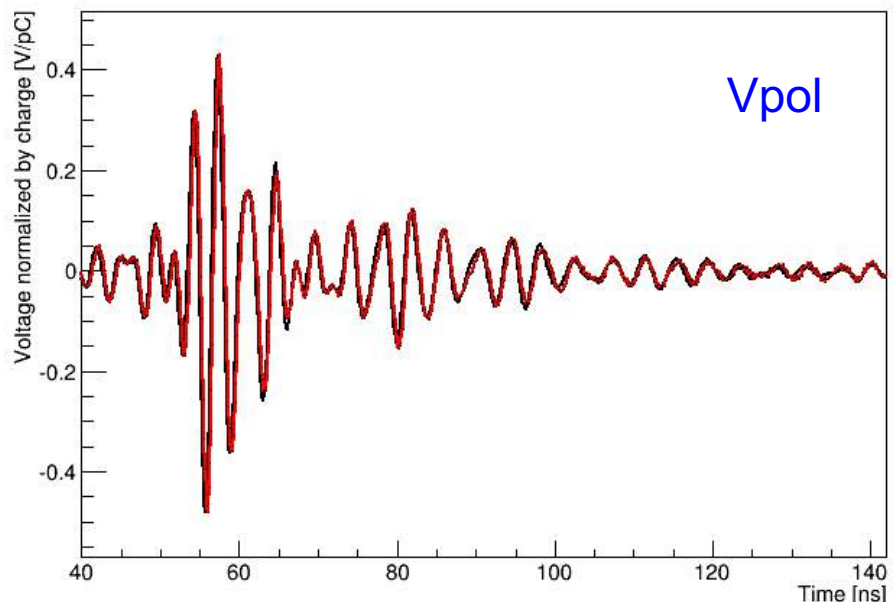
Reproducibility

The reproducibility was checked with data with the same configuration

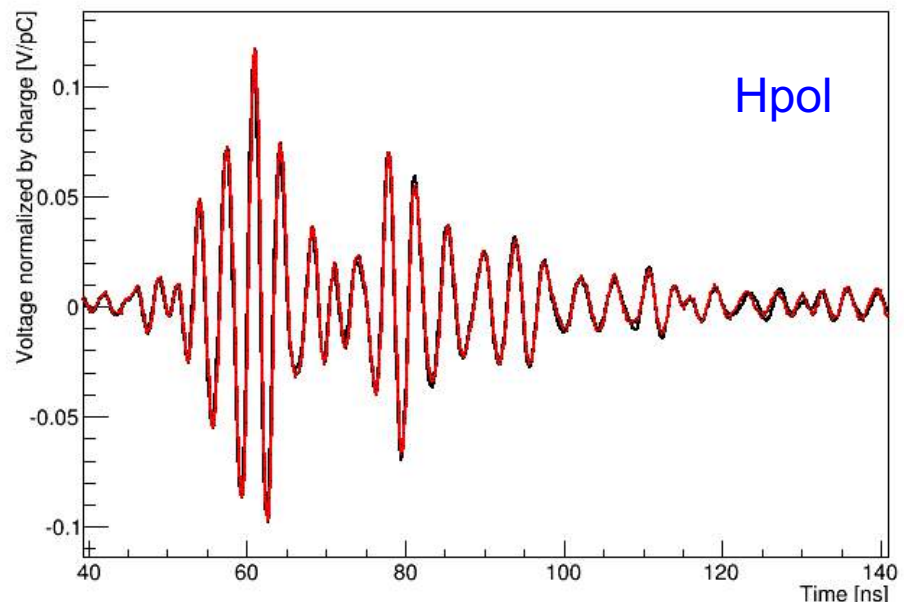
2015/01/14 Run1 (ice 60 deg., 0m)

2015/01/14 Run4 (ice 60 deg., 0m)

Waveform



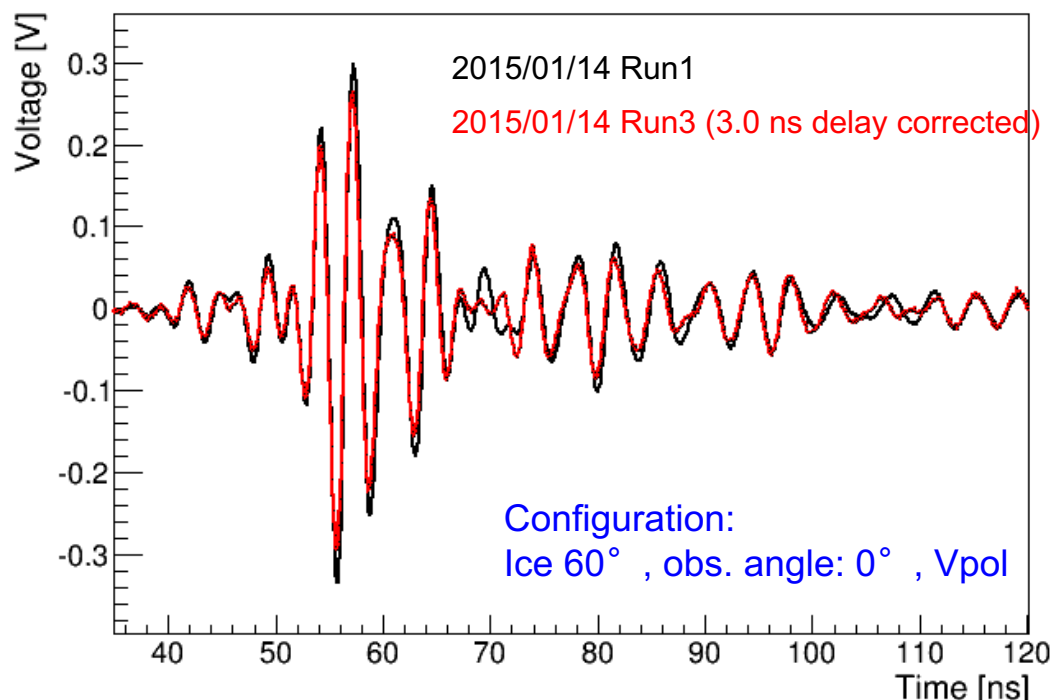
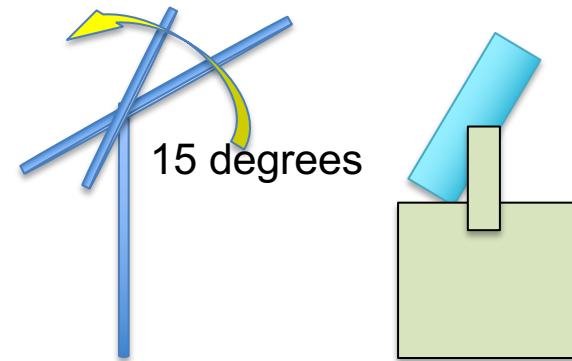
Waveform



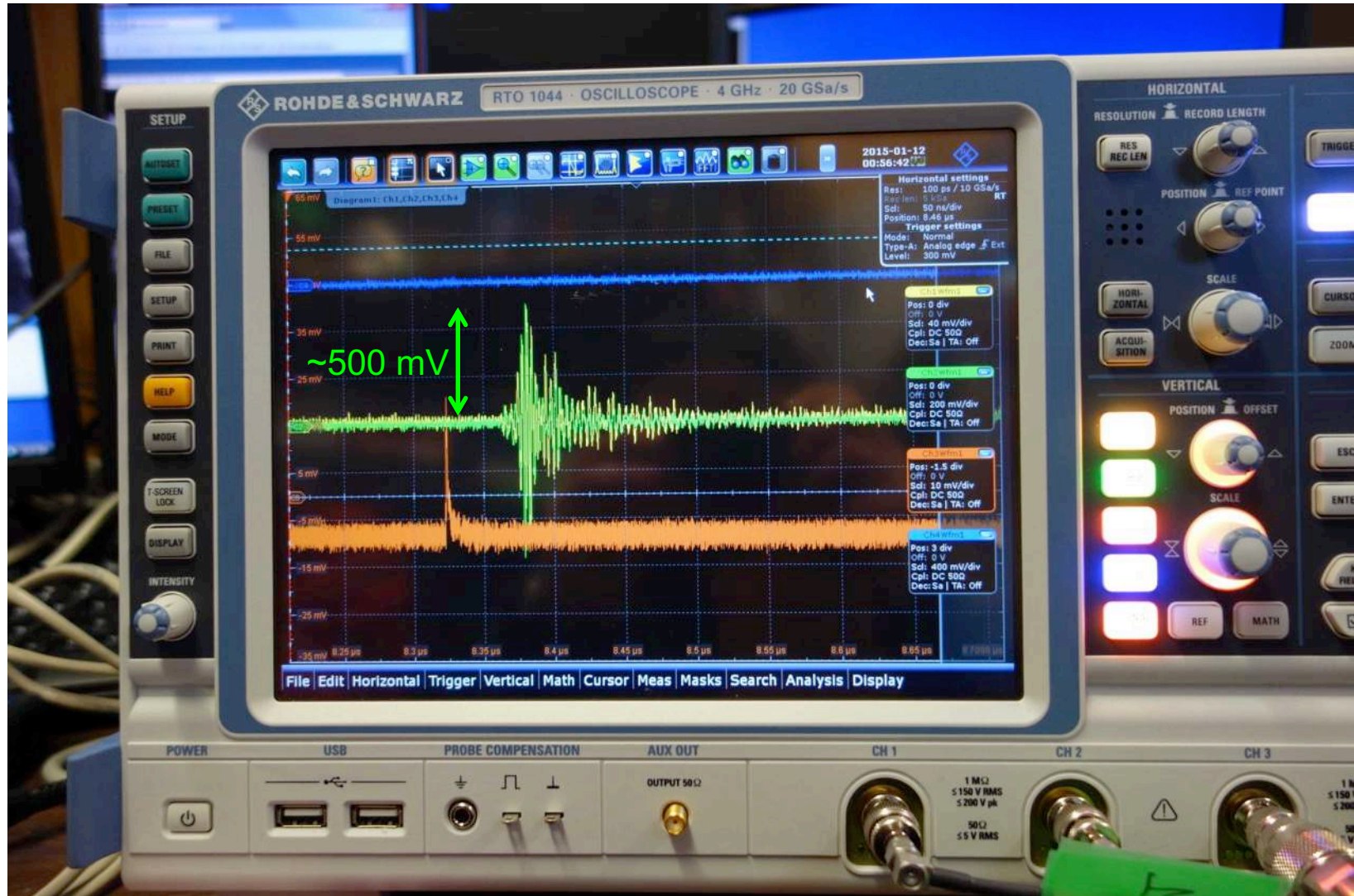
The difference in the amplitude is 5% → 10% in power (Vol)

■ Stability and far field confirmation

- ✓ The stability with the same configuration: 5% in amplitude
- ✓ The antenna mast was intentionally rotated by ~ 15 deg.
- ✓ The signal amplitude decreased proportionally with the distance change. → Far field confirmation (3.0 ns time delay → 12% distant → 12% amplitude decrease)
- ✓ Time difference from the expectation was checked for each configuration.
- ✓ The spread is 1.9 ns → 9° rotation → 8% in amplitude
- ✓ The overall systematic uncertainty in power: 19%

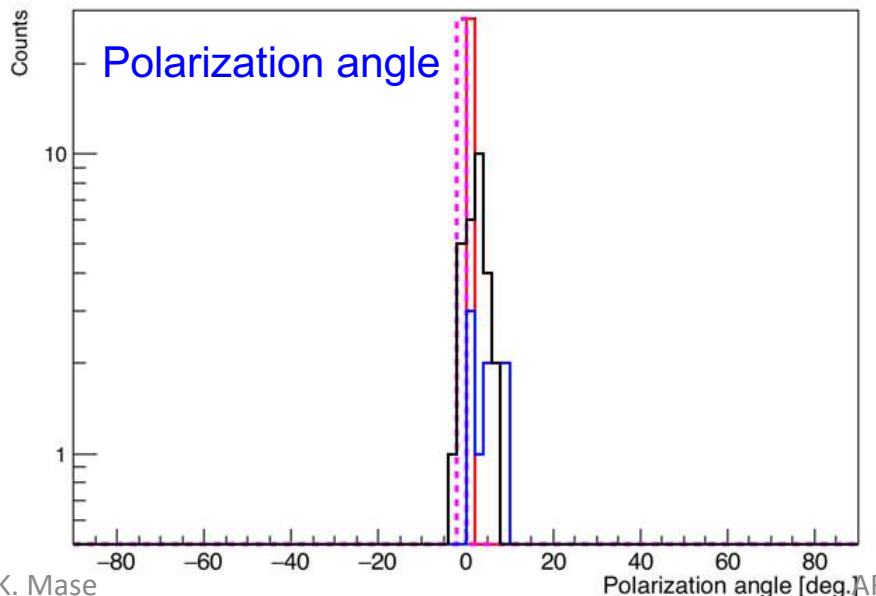
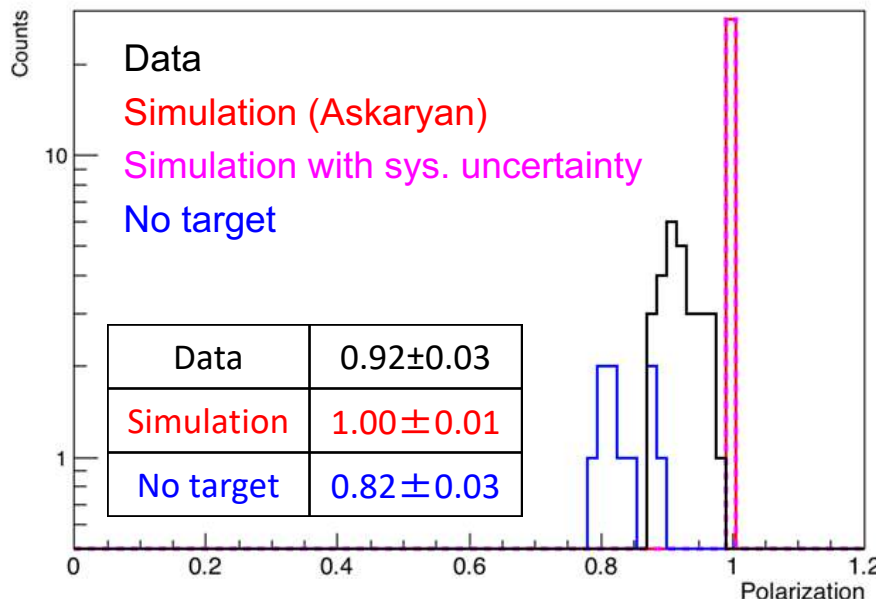


Signals observed!



Polarization

Polarization

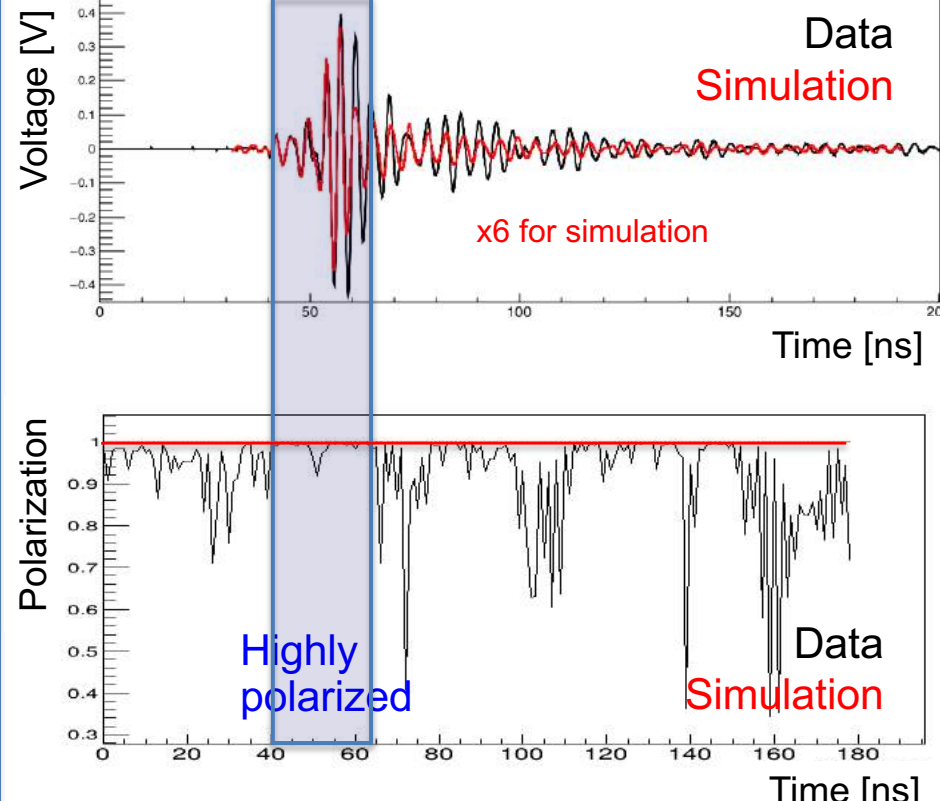


K.

Mase ARENA 2018

Time development of polarization

Configuration: Ice 30° , obs. angle 0° ,
Vpol

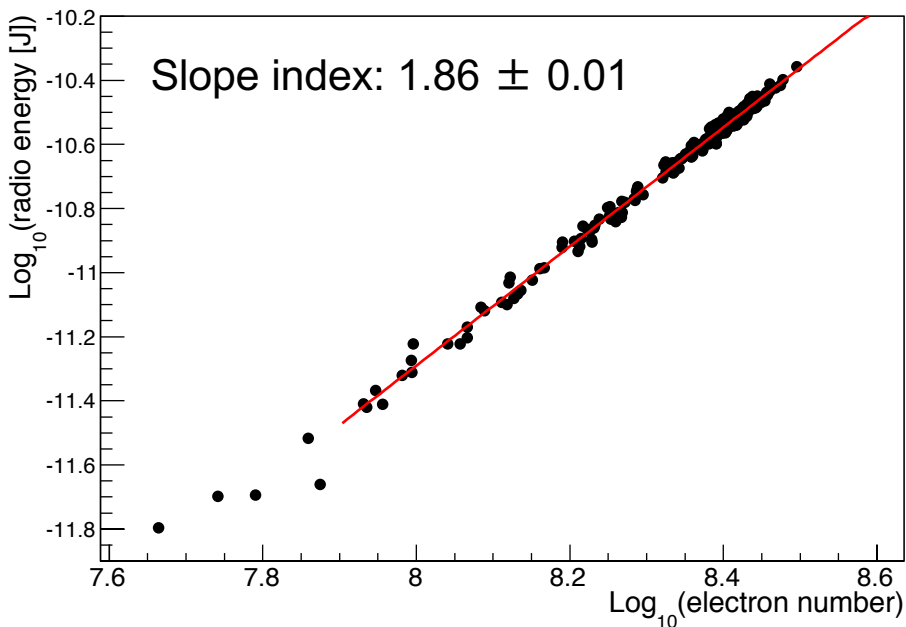


- ✓ All signals shows high vertical polarization
- ✓ Data is off from simulation

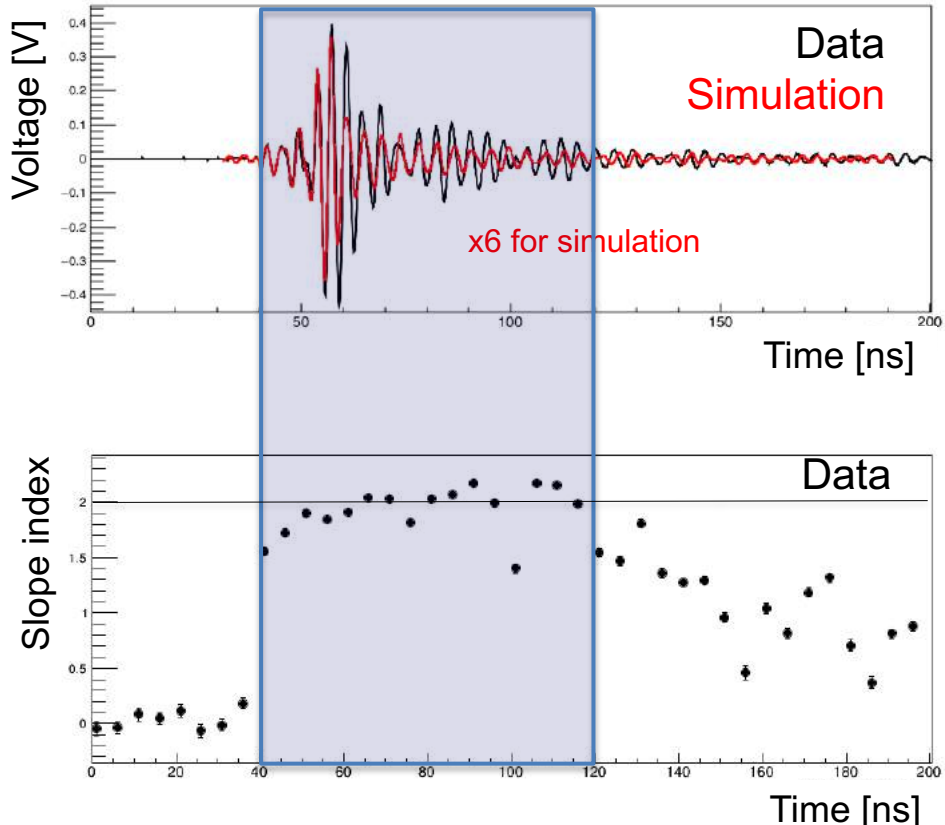
Coherence

Time development of coherence

Configuration: Ice 30° , obs. angle 0° ,
 Δpol



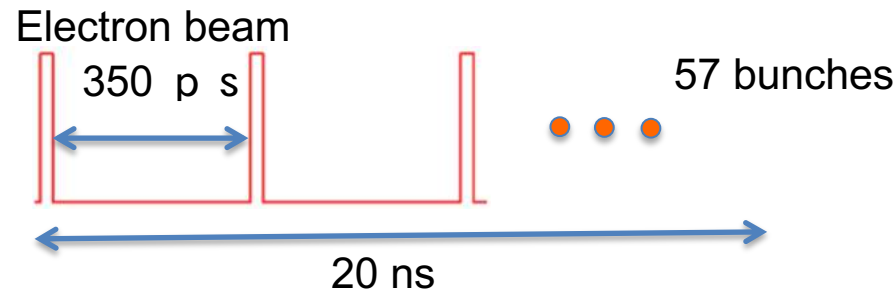
High coherence, but not full



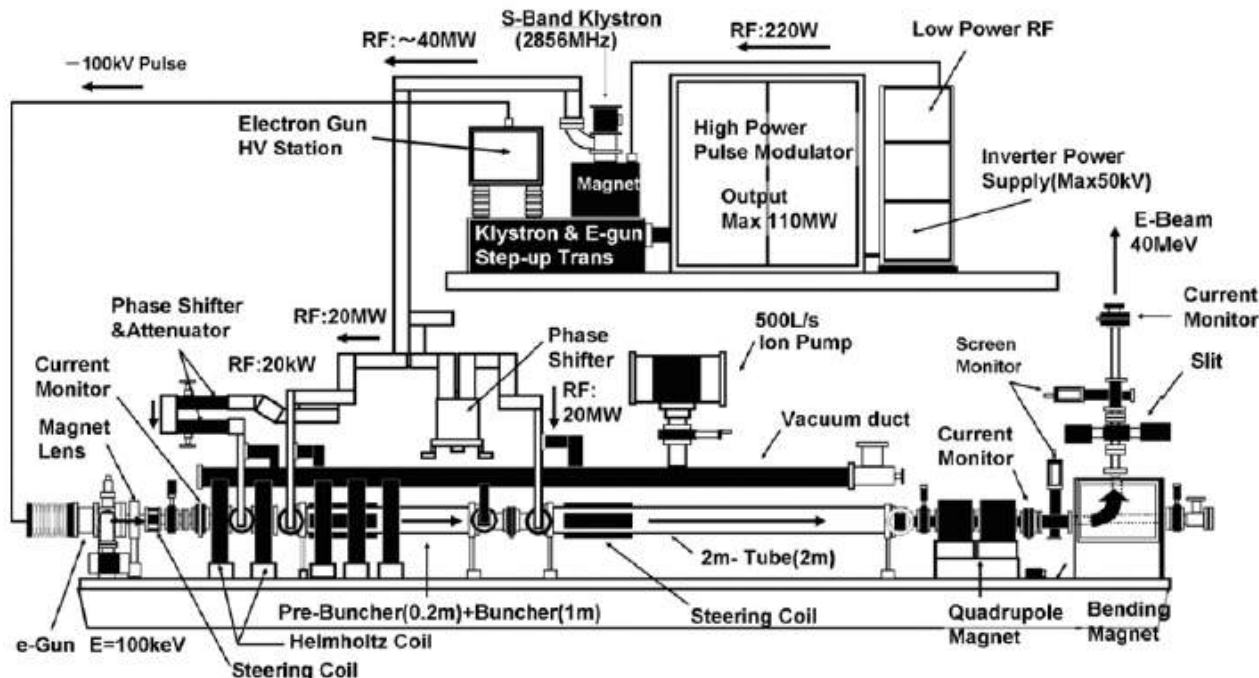
High coherence over the main waveform

TA LINAC

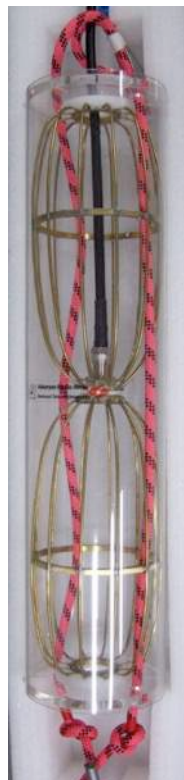
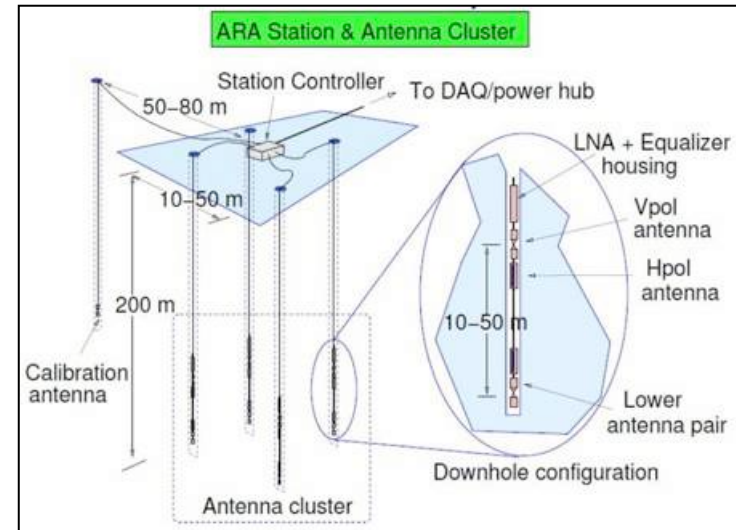
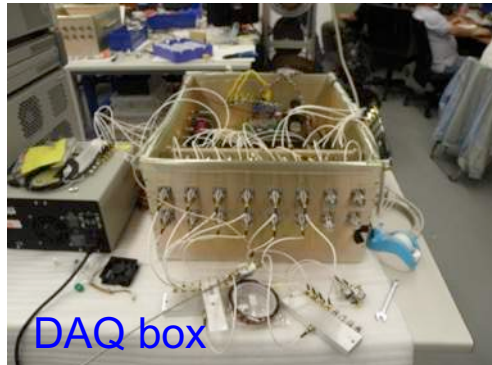
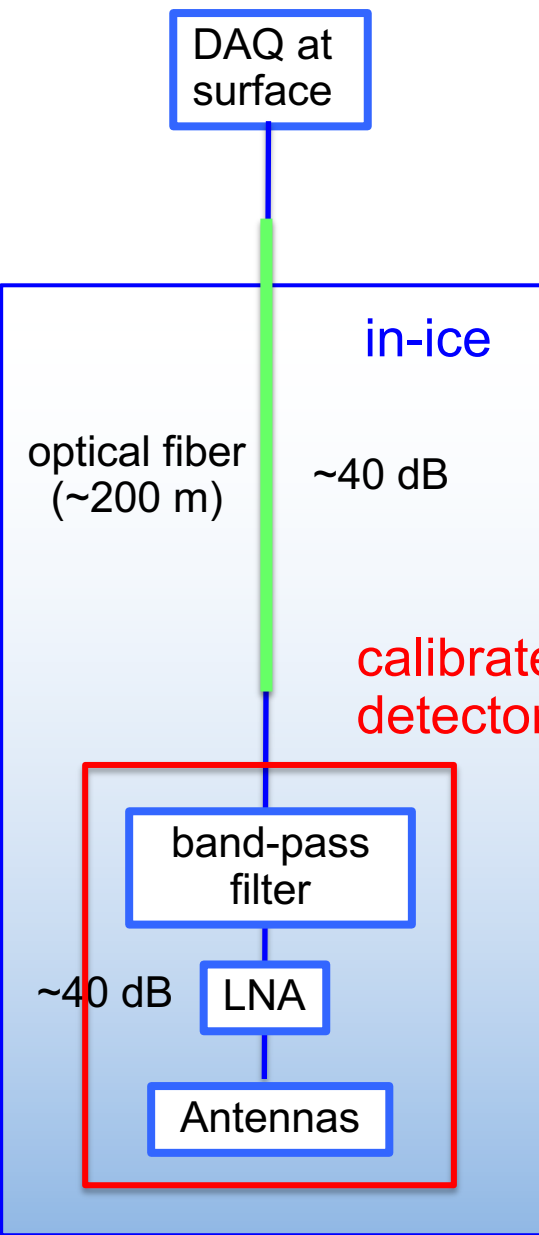
- ✓ 40 MeV electron beam
- ✓ Maximum electron number per bunch: 10^9
- ✓ Pulse frequency: 2.86 GHz
→ pulse interval: 350 ps
- ✓ Bunch duration is 20 ns
- ✓ Output beam width: 7 mm
- ✓ Trigger signal available



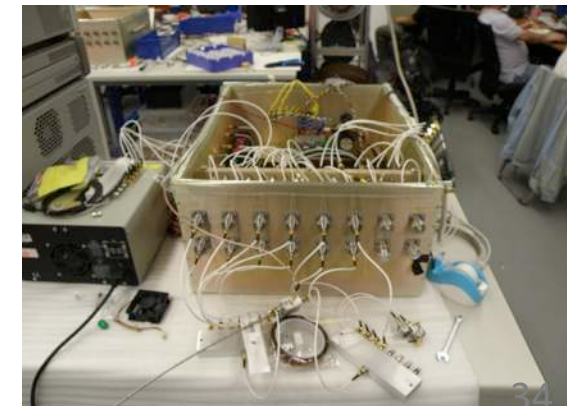
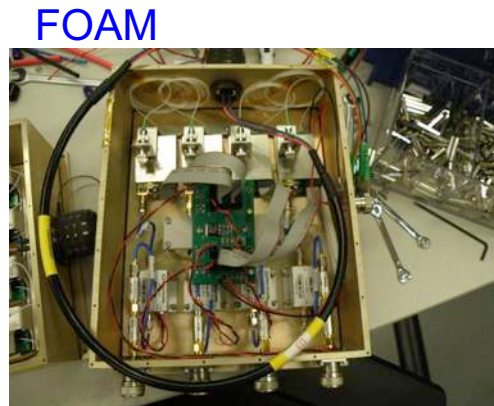
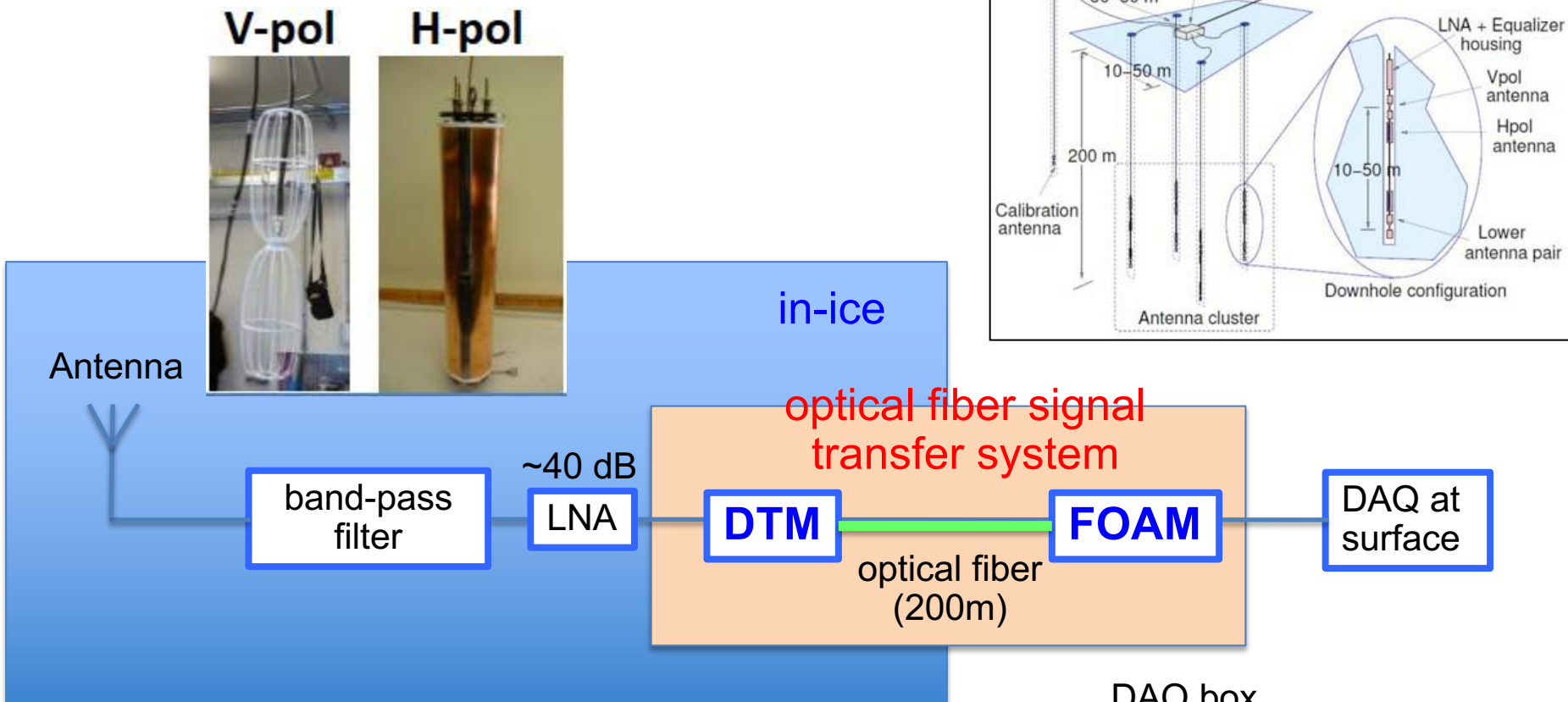
T. Shibata et al., NIMA 597 (2008) 61



The ARA system



Schematic of the ARA system



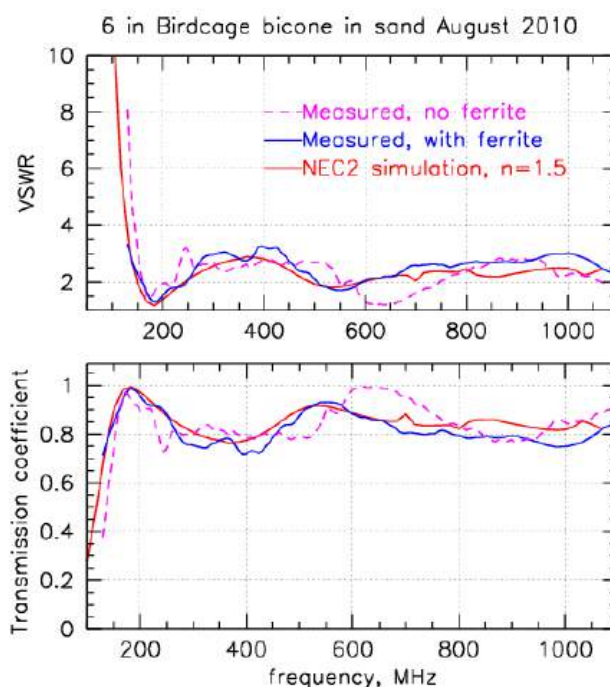
■ Antennas



V-pol antenna

Bicone

150-850 MHz

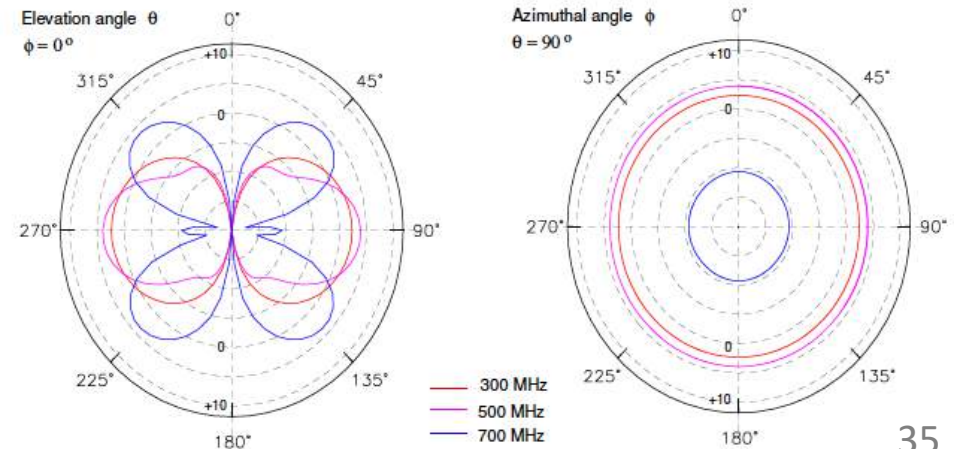


H-pol antenna

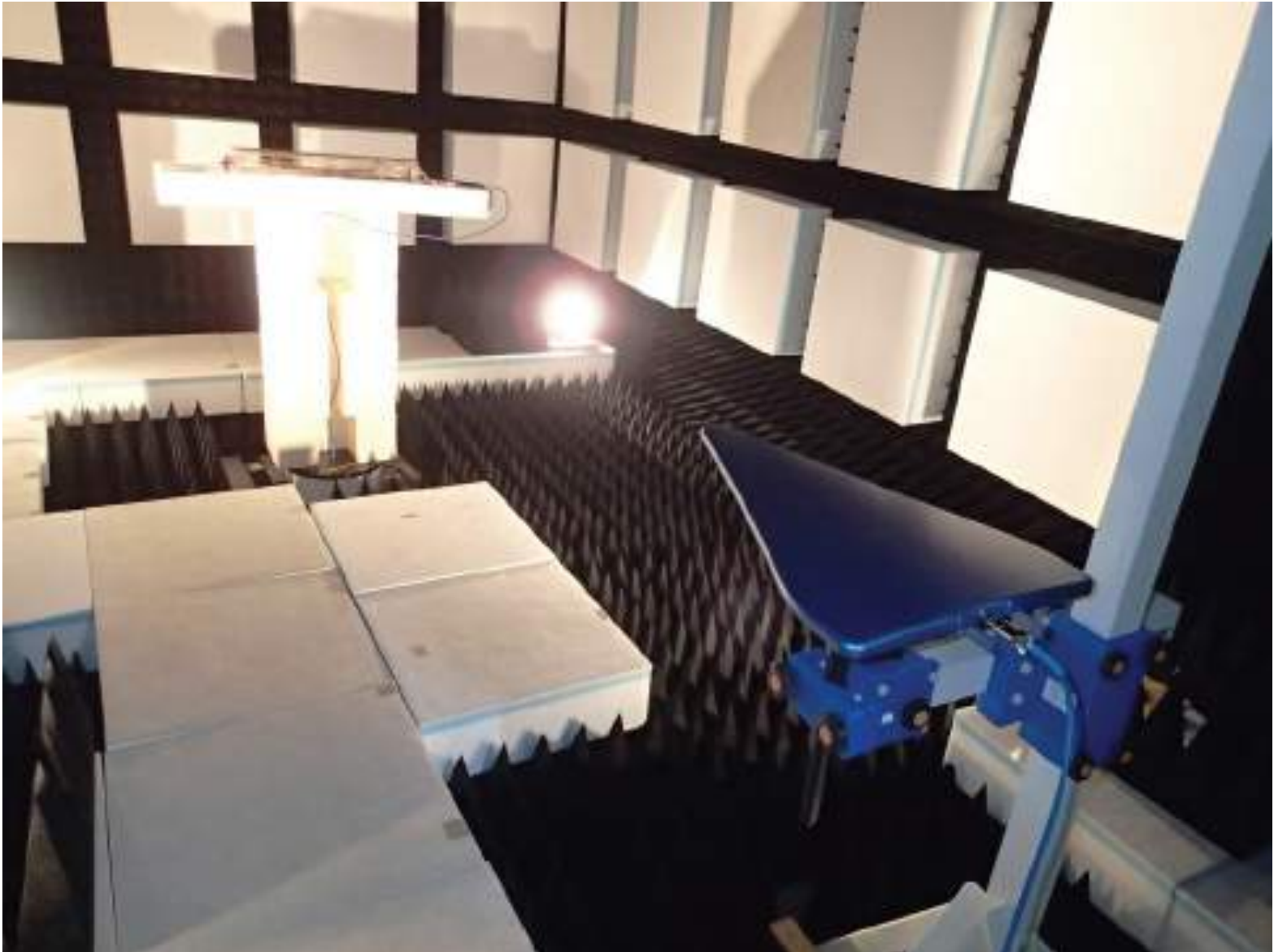
Quad-slot cylinder

200-850 MHz

Gain similar to dipole
(+2 dBi)

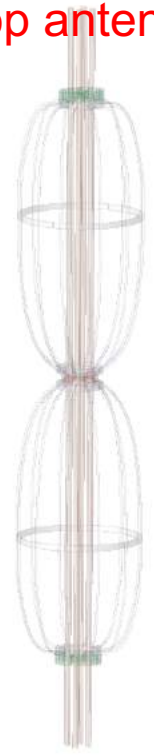


■ Antenna calibration



Antenna transmission coefficient

Top antenna



Bottom antenna

